International Journal of Biological Macromolecules 319 (2025) 145372

Contents lists available at ScienceDirect

International Journal of Biological Macromolecules

journal homepage: www.elsevier.com/locate/ijbiomac

Deposition of alginate-oregano nanofibres on cotton gauze for potential antimicrobial applications

Abimbola Oluwatayo Orisawayi [a,b], Hao Lu [a], Ishrat Jahan Badruddin [a], Prabhuraj D. Venkatraman [c], Nicole S. Britten [d], Jonathan A. Butler [d], Krzysztof Koziol [a], Sameer S. Rahatekar [a,*]

[a] Composites and Advanced Materials Centre, Faculty of Engineering and Applied Sciences, Cranfield University, Bedfordshire MK43 0AL, United Kingdom
[b] Department of Mechanical Engineering, School of Engineering and Engineering Technology, Olusegun Agagu University of Science and Technology (OAUSTECH), Okitipupa, Nigeria
[c] Manchester Fashion Institute, Faculty of Arts and Humanities, Manchester Metropolitan University, Cavendish Street, Manchester M15 6BH, United Kingdom
[d] Department of Life Sciences, Faculty of Science and Engineering, Manchester Metropolitan University, Chester Street, Manchester M1 5GD, United Kingdom

ARTICLE INFO

Keywords:
Electrospinning
Nanofibre
Alginate
Oregano essential oil
Antibacterial bandages

ABSTRACT

In this study, we developed an innovative natural antibacterial medical bandage composed of electrospun nanofibres derived from alginate (SAg) and oregano essential oil (OEO). The nanofibre deposition process was systematically optimised, achieving a controlled evolution of fibre formation at intervals of 1, 2, 3, 4, and 8 h. Over time, fibre morphology has changed from a dispersed network to a densely packed, homogeneous, fibrous, fully embedding cotton gauze nanofibre. Scanning Electron Microscopy (SEM) revealed nanofibres with diameters ranging from 100 to 300 nm, 46 % measuring 100–200 nm, 37 % at 200–300 nm, and 14 % between 300 and 400 nm. Thermogravimetric Analysis (TGA) confirmed improved thermal stability in cross-linked samples. At the same time, Fourier Transform Infrared Spectroscopy (FTIR) shows the incorporation of OEO into the nanofibres shows OEO carvacrol, and thymol. Antibacterial efficacy tested inhibition zone assays against Methicillin-resistant *Staphylococcus aureus* (MRSA) and *Listeria monocytogenes* on double-layered bandages is 15 mm and 10 mm, respectively. Statistical analysis results from ANOVA confirmed that multi-layered bandages (TL-BSS) had significantly enhanced antibacterial activity compared to single-layered (SSS) and both-sided spun (BSS) configurations. Unlike conventional wound dressings, this study introduces a bioactive, nanofibre-integrated gauze with sustained antibacterial efficacy.

1. Introduction

The global increase in demand for advanced wound dressing materials has led to considerable research in developing more effective and sustainable wound healing treatments [1–3]. The World Health Organisation (WHO) reports that approximately 5 million of the 58 million people injured annually die from fatal wound injuries, while millions more suffer due to inadequate wound care, highlighting the urgent need for innovative wound-dressing technologies in biomedical engineering [4–6]. Non-healing wounds are a problem area that affects millions of people's quality of life and has caused significant clinical challenges that need to be addressed [7,8]. The skin is also an essential part of the body with multiple roles, including protection, [9] sensation [10], immunity, communication [10], and many other functions [11]. In recent years, traditional skin wound healing treatments have gained global interest. Studies have demonstrated that natural and extracted products, such as *aloe vera* [12], turmeric and curcumin [13], garlic [14], moringa leaves, seeds, and their oil, and oregano oil [15–17] are popular and have been proven effective in wound healing.

However, traditional wound healing methods face challenges such as a lack of standardisation, scientific validation, contamination risks, allergic reactions, medication interactions, and poor regulatory oversight. Addressing these through improved designs of bandages, sponges, films, and nano-/microfibres is key to advancing therapeutic technologies. [18,19]. Notably, recent studies have demonstrated the potential of electrospun nanofibres functionalised with bioactive agents for improved wound healing [20,21]. Advances in polymeric nanofibre-based wound dressings focus on materials like polyurethane,

* Corresponding author.
E-mail address: S.S.Rahatekar@cranfield.ac.uk (S.S. Rahatekar).

https://doi.org/10.1016/j.ijbiomac.2025.145372
Received 10 August 2024; Received in revised form 3 June 2025; Accepted 17 June 2025
Available online 18 June 2025
0141-8130/© 2025 The Authors. Published by Elsevier B.V. This is an open access article under the CC BY license (http://creativecommons.org/licenses/by/4.0/).

polycaprolactone, and polyvinyl alcohol for their tunable mechanics and drug release; however, These systems often rely on synthetic polymers, which, although advantageous for their tunable mechanical strength and controlled drug release, inherently lack the hydrophilicity, biocompatibility, and biodegradability characteristic of natural polysaccharide-based alternatives [22–24] Studies show that traditional dressings often cause dehydration and wound adhesion, leading to pain and delayed healing [24] While current dressings are absorbent and help prevent infection, they play a passive role in healing. However, incorporating novel composites can enhance antimicrobial activity and localised antisepsis, improving healing outcomes [4].

Electrospinning has continued to gain popularity due to its innovative and advanced engineering and manufacturing processes, which enable the formation of micro- and nano-structured composites from polymer solutions, provide tunable morphology, offer high surface area, facilitate drug delivery, and allow manufacturing control. [16,25]. Electrospinning enables the production of low-toxicity materials through easy control of process parameters [26]. They are used for Polymer-based nanocomposites and have found diverse applications in modern technology, ranging from energy storage [27,28] to biomedical systems. This versatility underscores their potential as platforms for multifunctional applications, including antimicrobial wound dressings, making it suitable for modifying existing and newly developed products. The unique properties of electrospun nanofibers can improve localised, controlled drug delivery at the wound site, achieving antimicrobial compound release during the wound healing process [29]. Abedi et al. [30] reported that electrospun chitosan-based scaffolds containing conductive polymers such as PEDOT: PSS exhibited improved mechanical properties and biocompatibility, making them suitable for tissue engineering applications.

Integrating bioactive compounds into electrospun nanofibers has been studied to enhance their antimicrobial and wound-healing potential. For instance, Lamei and Hasanzadeh [31] successfully incorporated metal-organic frameworks (MOFs) into electrospun nanofibres, significantly improving their wettability, haemostatic efficiency, and antibacterial activity. This approach aligns with fabricating electrospun materials for wound healing through controlled antimicrobial release. The use of naturally-derived materials such as alginate [32], chitosan [33], collagen [34], fibrinogen [35], fibrin [36], cellulose [37], and gelatine [38]. They have been widely used, and their composites are emerging for several medical applications. Studies have highlighted that functionalising these biomaterials with bioactive agents can significantly improve their wound-healing efficacy [39]. Lamei and Hasanzadeh [33] demonstrated that chitosan-PVA nanofibrous scaffolds modified with tannic acid and metal-organic frameworks exhibited enhanced antibacterial activity, improved mechanical strength, and superior haemostatic properties. Inspired by this strategy, the present study investigates the integration of oregano oil within electrospun alginate nanofibers to develop an advanced bioactive wound dressing with prolonged antimicrobial effectiveness.

Among these materials, alginate is one of the primary sources of sustainable and renewable materials, and it is widely available and low-cost [15]. Alginate is one of the most prevalent naturally biodegradable polysaccharides derived from seaweed or brown Algae. Alginate has advantageous properties and is an antimicrobial when used in coatings, particularly for delaying microbial spoilage in food and reducing contamination from neuropathogenic microorganisms. It can also be blended with other antimicrobial agents to enhance efficacy [40,41]. Essential oils contain complex, volatile compounds synthesised by plants for protection and signalling, exhibiting physical, biological, and chemical properties beneficial as natural antimicrobials, anti-inflammatory, and antidiabetic agents, and for treating various medical conditions [42]. Among these essential oils is oregano essential oil (OEO), Carvacrol with smaller percentages of thymol, p-cymene, gamma-terpinene, and other trace compounds known for their promising and effective natural and sustainable antimicrobial activity [15].

The innovative approach in this study involves integrating electrospun sodium alginate (SAlg) and OEO nanofibres onto a cotton gauze bandage. Despite extensive studies on alginate and OEO separately, their electrospun integration onto cotton gauze bandages as a bioactive dressing remains unexplored [43]. Several works have been done to examine the potential biomedical applications of alginate, the antimicrobial properties of OEO, and the use of electrospinning for improving bandage functionality [44,45]. However, the integration of alginate, OEO, electrospinning, and bandages into a single functional wound dressing has not been extensively studied. This is the critical research gap in this field. Conventional cotton gauze dressings function passively, primarily offering wound coverage and absorbency, and often lack bioactive properties [46]. By incorporating electrospun alginate-OEO nanofibres onto gauze, this hybrid dressing enhances antimicrobial efficacy, ensures sustained drug release, and optimises wound healing. Encapsulation of OEO within alginate nanofibres improves its stability, mitigating the rapid degradation and volatility limitations associated with free-used essential oils [47]. Accordingly, this study seeks to address the identified research gap by evaluating the performance of electrospun alginate-OEO nanofibre-coated gauze bandages as an advanced wound dressing system.

Alginate and oregano essential oils (OEO) are widely accessible and cost-effective materials [48]. While cotton gauze remains highly affordable, particularly in low- and middle-income countries, it serves as a low-cost antimicrobial dressing that could enhance accessibility to wound care and provide a clinically relevant, cost-effective, and scalable solution across Africa and Asia, where access to quality wound care is limited [49]. The hybrid electrospun alginate-OEO nanofibres on gauze could offer positive moisture retention, improved bacterial inhibition, and controlled drug release, potentially reducing infection risks and fostering faster wound healing.

This study aims to develop a potential antibacterial wound dressing by integrating electrospun SAg and OEO nanofibres onto a cotton gauze bandage and evaluating its structural, thermal, and antibacterial properties. Specifically, this research aims to optimise the electrospinning process to achieve a controlled evolution of nanofibre formation on the cotton gauze, ensuring uniform deposition and enhanced surface interaction. Investigate the morphological, chemical, and thermal characteristics of the electrospun SAg-OEO nanofibers to assess their stability and functional properties using SEM, AFM, FTIR, and TGA. Evaluate the antibacterial efficacy of the electrospun bandages against *MRSA* and *Listeria monocytogenes* using inhibition zone assays and statistical analyses to determine their effectiveness. Compare nanofibre deposition configurations (SSS, BSS, and TL-BSS) to assess their impact on antimicrobial performance and wound-healing potential.

2. Experimental section

2.1. Materials

Sodium alginate (SAg), (SIGMA A2033, 9005-38-3, M/G ratio = 2.12, the viscosity of 1 % solution at 25 °C ~ 4–12 cP, ignition residue <30 %, molecular weight, 21,900 g mol^{-1}, loss on drying <15 %), (Procured from Sigma-Aldrich, MO, USA), Poly(ethylene oxide) Powder (CN 043678.14,-25322-68-3 Viscosity: 400 to 800 cps (2 % aq. solution, 25 deg. C), M.W. 1,000,000 Alfa Aesar, Procured from Thermo Fisher Scientific, Haverhill, MA, USA), Pluronic® F-127 powder (PL, SIGMA P2443, product of Sigma-Aldrich, MO, USA), calcium chloride ($Cacl_2$) (procured from Fisher Scientific, Loughborough, UK), The oregano oil used in this study is (100 %) essential oregano oil *Origanum vulgare*, obtained from Athina Greece, with its primary constituents comprised of carvacrol, 80 %; thymol, 4.2 %; p-cymol, 4.2 %; gamma-terpinen, 1.6 %; limonen, 0.22 %; sabinen, 0.25 %; and linalool, 0.12 %; the rest of the components were <0.1 %. Reported from previous studies [15] (10 mL). For electrospinning deposition experiments, a non-elastic woven cotton gauze bandage (medical grade) was used. The bandage was obtained

from a trusted supplier in the UK.

2.2. Preparation of OEO/SAg and PEO solution

Solutions of Sodium Alginate (SAg) 3.5 wt% and Poly (ethylene oxide) Powder (PEO) 4 wt% were each prepared separately using deionised water. These were stirred at 200 rpm on a digital hotplate magnetic stirrer for 24 h at a temperature range (18–25 °C). The alginate and PEO solutions were mixed in an 80:20 weight ratio. The resulting solution was mixed with 1 % of Pluronic® F-127 as a surfactant, and the OEO content was carefully adjusted during the solution preparation process. The content was controlled to a specific weight percentage relative to the dissolved alginate polymer during solution preparation, 2 wt%, determined through preliminary experimental investigations to enhance compatibility within the nanocomposite matrix [15]. This mixture was stirred at 200 rpm for approximately 12 h until it was entirely homogeneous (uniform dissolution), a slightly yellowish, observable solution. The solution was transferred into a 10 mL syringe and placed inside a beaker, which was then positioned in a vacuum oven to remove any visible bubbles gradually.

2.3. Electrospinning process

Before beginning the electrospinning procedure, the non-elastic cotton medical bandage was attached directly to the metal board on the surface of the collector machine collector plate. The electrospinning was conducted on, Bioinicia LE-50 FLUIDNATEK™, an advanced benchtop machine (Valencia), Spain. Electrospinning parameters were set up considering earlier studies on nanocomposite fibres developed from a blend of oregano oil and alginate [15]. With slight variation in the parameters as follows: distance from the collector surface to the needle tip at 15 cm, and the flow rate ranges between 1.0 and 1.2 mL/h; fibres were developed using a voltage range of 24 to 30 kV, within a temperature range of 18 °C to 25 °C, at a relative humidity of 40 % to 60 %, with a needle diameter of 0.4 mm, The objective was to develop a stable production of alginate–oregano oil nanofibres deposited on the cotton bandage. Experimental improvements were conducted to perfect the growth of electrospun alginate–oregano oil fibres on the surface of the bandage. Five samples were collected at one-hour intervals, up to four hours, with the final sample undergoing electrospinning for approximately 8 h. Fig. 1 shows the electrospinning setup for producing alginate-oregano nanofibres deposition on cotton gauze. This setup investigates the practical application of incorporating SAg and OEO nanofibre, previously developed by Lu et al. [15] to modify the bandage.

2.4. Cross-linking and preparation for characterisation

Cross-linking refers to the process where chemical bonds are formed between polymer chains, which helps in enhancing the polymer's stability and strength [15]. Fig. 2a-c shows pictorial electrospun alginate-oregano oil deposition nanofibres on the bandages of the uncross-linked bandage (UcB), the cross-linking process of bandage showing the immersion in calcium chloride solution, and the cross-linked or the modified (MoB) and dried cotton gauze bandage, with visible structure of the modified bandage after soaking in water. The cross-linking process has two main steps (i) immersion of the nanofibre-coated bandage in 4 wt% $CaCl_2$ solution to enable ionic cross-linking of alginate with calcium ions, and (ii) rinsing the sample in deionised water to remove unbound PEO and residual salts. First, 4 wt% calcium chloride solution was prepared with deionised water. The bandage with the nanofibres was removed from the collection board and then immersed in the calcium chloride solution for 30 min. During this period, turning over the bandage properly was necessary to ensure that the fibres on both sides of the bandage were fully cross-linked with the calcium ions in the solution. After the cross-linked sample was soaked in deionised water for 24 h. This step effectively removed the PEO that could not be cross-linked

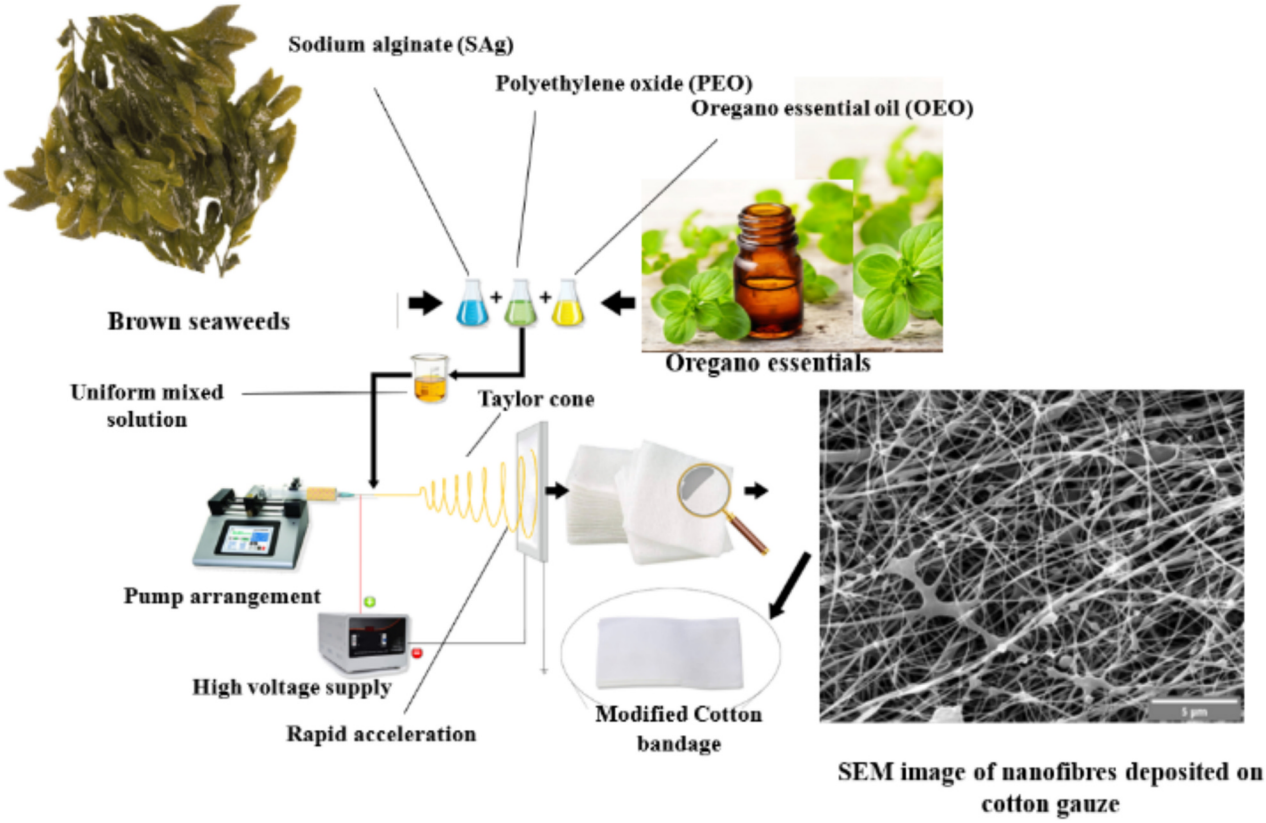


Fig. 1. Electrospinning setup for producing alginate-oregano nanofibres deposition on cotton gauze.

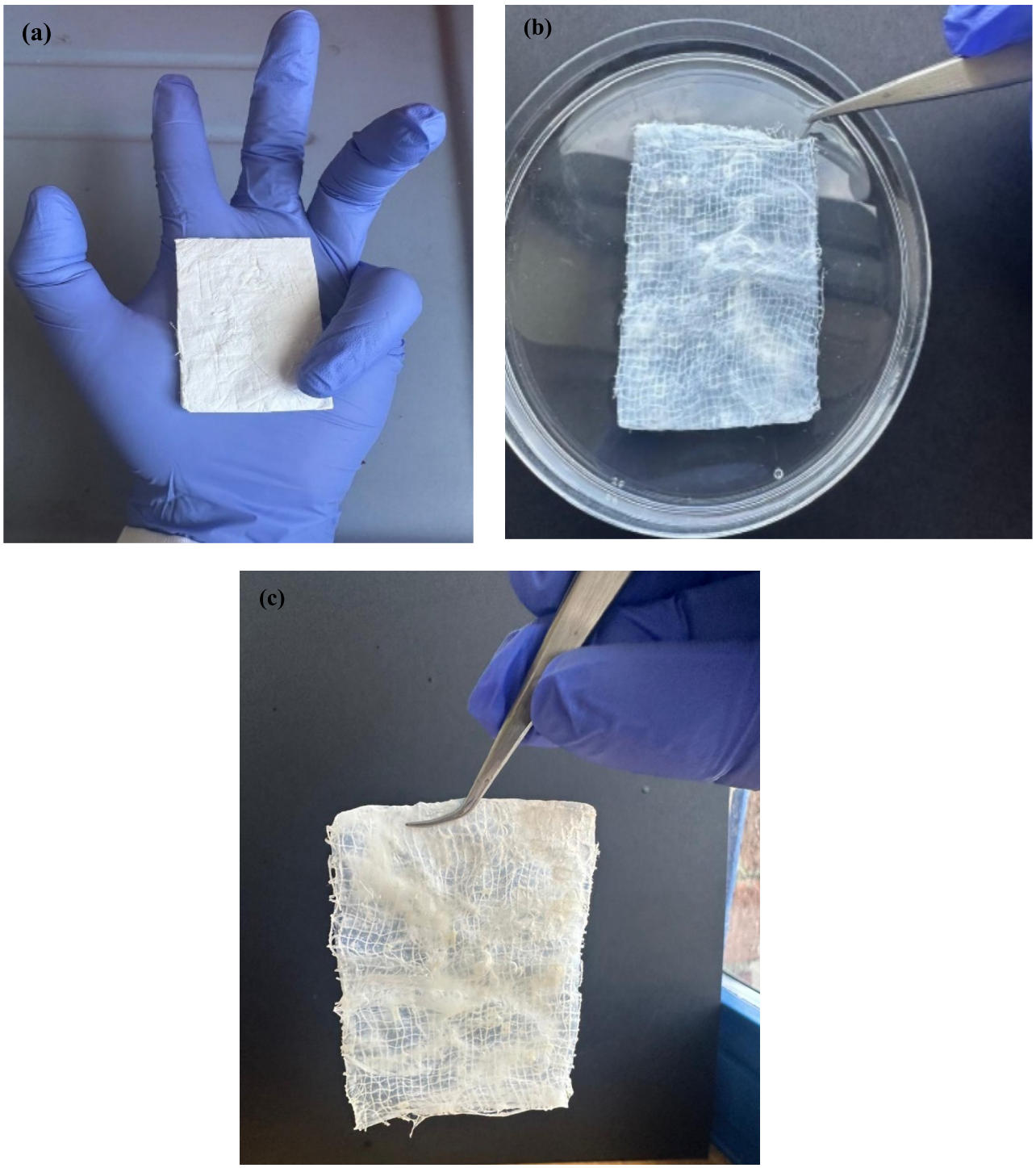


Fig. 2. Electrospun alginate-oregano oil nanocomposite bandages (a) uncross-linked flexible bandage (UcB) was coherent and structured nanofibrous networks (b) cross-linking process of the bandage during immersion in 4 % $CaCl_2$ solution (c) cross-linked or modified (MoB) and dried cotton gauze bandage, visible with a heterogeneous distribution of the deposition of nanofibrous network after soaking in water.

and residual calcium chloride from the sample surface. It was then dried under ambient conditions. Using a Gallenkamp TH 340 l/−40 °C chamber capable of conditioning samples at a temperature range of between −40 and 180 °C, the temperature was regulated between 21 °C and 25 °C and humidity at 45 % for 24 h. These controlled conditions ensured reliability and reproducibility, there was a need to maintain the constant weight of the samples, and this was done [50]. The electrospun alginate fibres existed in a stabilised form with potential encapsulation of oregano essential oil (OEO) within the alginate matrix or in localised pockets. To minimise OEO vaporization loss during storage, the alginate-modified cotton bandages were immediately sealed in airtight plastic zip-lock bags after the manufacturing process. This approach ensured that the OEO content in the final samples closely reflected the original weight fraction specified during solution preparation.

3. Instrumentation and characterisation

3.1. Morphology characterisation of the bandage

Before observing the samples on the Environmental Scanning Electron Microscope (ESEM), each, including the unmodified bandage (UmB), uncross-linked modified bandage (UcB) and cross-linked or modified bandage (MoB), was coated with a gold layer, specified as AU10, to improve conductivity and prevent charging during SEM imaging. Based established in prior studies, thin sputter coating 10 nm for surface morphology and fibre diameter interpretation, ensuring accurate qualitative and quantitative assessment [15,16]. The structured and morphological characteristics of the fibres on these bandages were examined using an Environmental Scanning Electron Microscope (TESCAN S8000), Kohoutovice, Czech Republic. During analysis, Image editing was conducted using Photoshop to segment the images into 25 distinct grids, followed by detailed analysis, using Image J and Diameter J software to assess fibre dimensions and uniformity.

3.2. Topography characterisation of the bandage

The 3D high-resolution surface topographic imaging analysis of uncross-linked modified bandage (UcB) and cross-linked modified bandage (MoB) was conducted on Bruker Dimension 3100 Atomic Force Microscope (AFM) instrument, equipped with a *V* controller nasoscope and PPP-NCHR tip with silicon nanosensors in tapping mode was used to conduct the 3D resolution. The can size was 20 by 20 μm with a depth rate range of 1 to 30 μm, a scan speed frequency of 0.4000 Hz, and the drive amplitude was set to 123.7 mV, with an operating resolution of 1024 lines per 1024 samples per line using zero crossing to identify where the surface profile crosses the mean line and peak threshold value of 25.0 %. These settings were used to achieve an optimised value with the highest resolution necessary for evaluating detailed topography analysis properties of the uncross-linked modified bandage (UcB) and cross-linked or the modified bandage (MoB).

3.3. Characterisation of materials by FTIR spectroscopy

Fourier Transform Infrared (FTIR) spectroscopy was performed to analyse the samples of pure Oregano Essential Oil (OEO), Sodium Alginate (SAg), and the uncross-linked and cross-linked modified bandage (UcB & MoB), respectively. The characterisation was conducted using a Nicolet iS10 FTIR Spectrometer, equipped with an Attenuated Total Reflectance (ATR) accessory Smart iRT, Thermo Fisher Scientific™, Verona, (Madison), USA. Spectra were collected with a wavenumber range of 4000 to 500 cm^{-1}, 50 scans at a resolution of 4 cm^{-1}, conducted at room temperature using OMIC Software as recommended by the equipment manufacturer. Further data analysis was conducted using Microsoft Excel software.

3.4. Thermal analysis of alginate and the bandage

Thermogravimetric analysis (TGA) was used to assess the thermal stability and decomposition properties of uncross-linked bandage (UcB), and cross-linked or modified bandage (MoB). The characterisation was conducted using a TGA Q500-(complete@Enesi) Thermogravimetric Analyser Nbr from TA Instruments, Laboratory Equipment USA. The universal Analysis software was used. Approximately 5 mg of each sample was accurately weighed in the platinum pan. The temperature was ramped at a steady heating rate of 10 °C/min from 25 to 800 °C under a procedural mode of 1000 °C, Nitrogen gas was used as the balance Purge gas flow at 40 mL/min, and Sample purge gas flow at 60/min to prevent oxidation, and decomposition properties being measured. The equipment is efficient, with an air-cool time of 10 mins.

3.5. Antibacterial assays of electrospun alginate/OEO nanofibre bandages

The modified bandage samples were prepared into three distinct configurations based on the electrospinning deposition: single-sided spun (SSS), both-sided spun (BSS), and two-layered both-sided spun (TL-BSS). The SSS were the samples on which electrospinning was performed on only one surface of the bandage substrate for 4 h, ensuring uniform nanofiber deposition on a single side. BSS were sampled, and electrospinning was applied to both sides of the bandage substrate for 4 h per side (total 8 h). The TL-BSS two BSS samples were stacked to form a multilayered structure. Bacterial cultures of *Methicillin-resistant Staphylococcus aureus* strain USA300 (MRSA) and *Listeria monocytogeens* strain Scott A were grown on Mueller-Hinton agar (Oxoid, UK) for 24 h at 37 °C. Agar plates were inoculated with bacteria adjusted to a Macfarland standard of 0.5, and 6 mm circular discs of each modified bandage material were applied to the bacterial plates. Cultures were incubated for a further 24 h at 37 °C, and zones of bacterial growth inhibition around the target samples were measured using a digital calliper gauge to ensure precision to identify antibacterial activity. Three independent measurements were taken for each sample, and the mean values were reported in millimetres (mm).

3.6. Antibacterial evaluation with statistical analysis

A one-way ANOVA was conducted to determine if there were statistically significant differences in the antibacterial effectiveness by increasing the number of different sample configurations (SSS, BSS, and TL-BSS) against *MRSA* and *L. monocytogenes*. Tukey's multiple comparison tests were used to determine pairwise differences between the sample configurations [51]. Error bars represent the standard error of the mean of $n = 3$ biological replicates. The analysis was conducted at a 95 % confidence level ($\alpha = 0.05$), considered statistically significant. The hypotheses evaluated were the null hypothesis (H_0): There is no significant difference in antibacterial inhibition among different sample configurations, and the alternative hypothesis (H_1): there is a significant difference in inhibition among sample configurations. The statistical analyses were performed using GraphPad Prism version 10.4.1, and histograms were plotted using Microsoft Excel.

4. Results and discussion

4.1. SEM assessment of UmB, UcB and MoB fibres

Fig. 3 illustrates typical SEM images of bandage development stages, with the initial unmodified bandage (UmB) (Fig. 3a_1 and a_2). The images in Fig. 3b-e are the images obtained from the SEM during the evolution of the fibre deposition at intervals of 1, 2, 3, and 4 h, respectively, demonstrating the evolution of fibre formation on the bandage over time. At 4 h (Fig. 3e), we achieved complete coverage on a single side of the bandage, and an additional 4 h of deposition was applied to each side to ensure thorough, even coverage across both surfaces. Fig. 3f and g shows the uncross-linked (UcB) fibre morphology and the cross-linked or modified (MoB) fibre, respectively. We have used this progressive fibre formation for up to 4 h to optimise the deposition evolution process, ensuring complete and even coverage at specified time intervals. The 8 h was achieved on the other side of the UcB and Fig. 3g for the MoB nanofibres on the bandage.

The SEM image of the unmodified bandage is in Fig. 3a_1 shows continuous images of threads composed of finer twisted fibres, which are large, loosely woven, and exhibit a natural, irregular twist shape. Fig. 3a_2 at a higher magnification, the surface of the ribbon-shaped cotton fibres is characterised by a smooth texture with some natural fibrillation similar to images obtained from yarn composites [52]. The diameter of the cotton threads was 200 μm (measured using ImageJ), and the diameter of the fine nanofibres that comprised the thread was

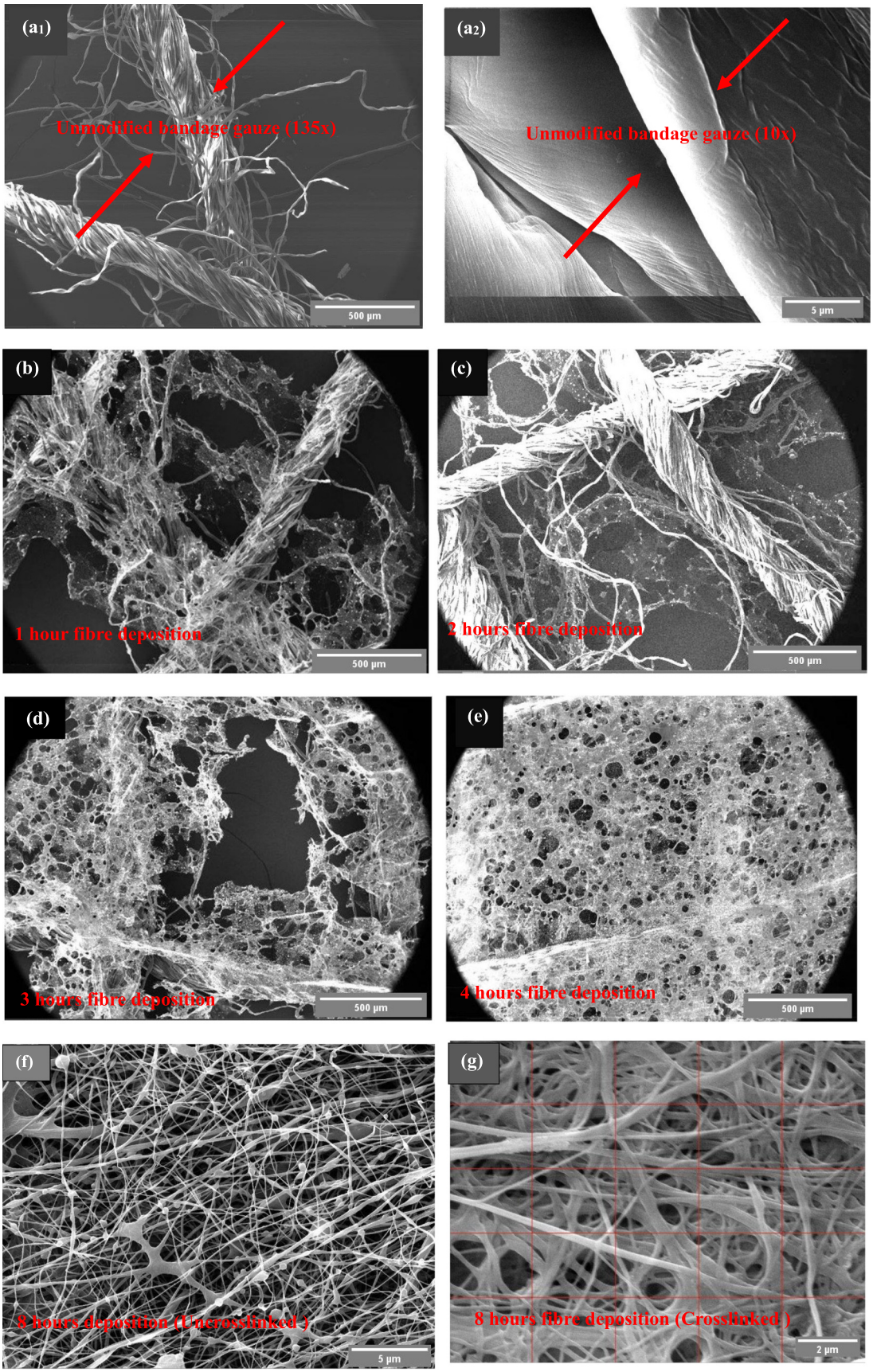


Fig. 3. SEM images of bandage development stages with Initial unmodified bandage shown at 135× and 10kx magnifications (a_1), (a_2); evolution of alginate–OEO nanofibres depicted at various electrospinning duration of 1 to 4 h at (b)-(e); UcB (f) and after and (g) MoB.

approximately 10–20 μm. The fibre smooth surface of the cotton gauze bandage could have minimal characteristic features for microbial interaction. [53,54]

The result from the fibre formation images of the modified bandage with alginate-OEO nanofibre filaments growing on the bandage fibres at each hour of electrospinning, as observed from the SEM images shown in Fig. 3b after 1 h of electrospinning resulted in initial layers of SAg-OEO nanofibres formation like thin films of nanofibres visible between the cotton fibres. In Fig. 3c after 2 h, gaps between the cotton are filled with more fibres, and the area of the nanofibre films between the cotton fibres gradually expanded until they were connected after 3 h of electrospinning. Further electrospinning for up to 4 h is observed to have covered the underlying cotton and reduced the visibility of the cotton fibres, as shown in Fig. 3e. After 4 h, the nanofibre mat was filled with abundant fibre-forming composites and wholly covered with SAg–OEO nanofibres composites.

The location of OEO within the alginate nanofibers can be understood based on the partially compatible molecular interactions between alginate and OEO from previous studies [15] which is like partially compatible polymer blends with essential oil in various studies [55,56], the alginate-OEO blend is expected to exhibit a morphology where OEO forms continuous domains distributed within the alginate polymer matrix [43]. This distribution is consistent with previous studies on partially compatible polymer blends, which serve as a basis for our assumptions [43,57]. This nanofibre mat could be crucial for effectively delivering the OEO during wound healing [58,59].

Fig. 3f and g shows the final SEM images of the enhanced bandage, representing the uncross-linked and cross-linked samples after electrospinning, respectively. The images indicate that the cotton fibre structures were no longer visible, suggesting that the SAg–OEO nanofibers effectively covered the bandage threads. However, as observed in Fig. 3f and g, SEM imaging does not provide sufficient contrast to definitively distinguish individual fibres at specific scales. Despite this limitation, the nanofibers appear well distributed across the bandage surface, supporting the inference of adequate coverage. The OEO has been encapsulated or packed into the alginate matrix; the OEO cannot be directly visualised as discrete droplets in the SEM images. This is due to the homogeneous nature of the solution during preparation, which prevents phase separation that would result in distinguishable oil domains. Instead, the encapsulation of OEO within the nanofibers is inferred from the morphological uniformity observed in the SEM images and supported by prior studies on polymer-essential oil interactions [60]. The final image diameter distribution derived from the SEM images of the modified bandage after cross-linking, soaking in water, and drying up in the air shows a clear indication of how the bandage SAg–OEO was distributed. Details on the diameter distribution of the nanofibres shown in Fig. 4 explained that the diameter of most fibres was between 100 and 300 nm; 46 % of fibres had a 100–200 nm diameter, and 37 % had 200–300 nm. There were some (14 %) fibres with a diameter between 300 and 400 nm. Very few fibres had diameters above 400 nm (2 %) and below 100 nm (1 %). This is a total of about 83 % within the optimal range. This diameter distribution could be beneficial or established to enhance surface area-related properties such as drug delivery and microbial interaction [61]. The findings suggest that cross-linking may have influenced the structural characteristics observed in our fabricated fibres, reinforcing the theoretical and practical applicability of such modifications for medical applications, particularly in wound care. Further insights into these effects are explored through AFM analysis, with comparisons to relevant literature with understanding these structural variations is also essential for evaluating fibre interactions with microbial agents and body fluids, which are critical considerations in biomedical applications [55].

4.2. Atomic force microscopy assessment (AFM) of the UcB and MoB

Atomic Force Microscopy (AFM) determines structures related to the 2-dimensional and 3-dimensional topography and the nuclear nature of surfaces [62]. Fig. 5 shows the 2-dimensional (2-D) and 3-dimensional (3-D) topography of the UcB and MoB after it has been washed, soaked, and dried. The images show observable features of the deposited nanofibres on the bandage. The nanofibres are observed as a combination of randomly distributed and homogeneous on the surface of the bandage in the image, which is in line with previous studies by Suganya and Stalin [63]. The cotton gauze bandage was covered entirely by electrospun nanofibre. The result obtained from the AFM shows an increase in the roughness value from about 149.5 nm in the UcB to 176.5

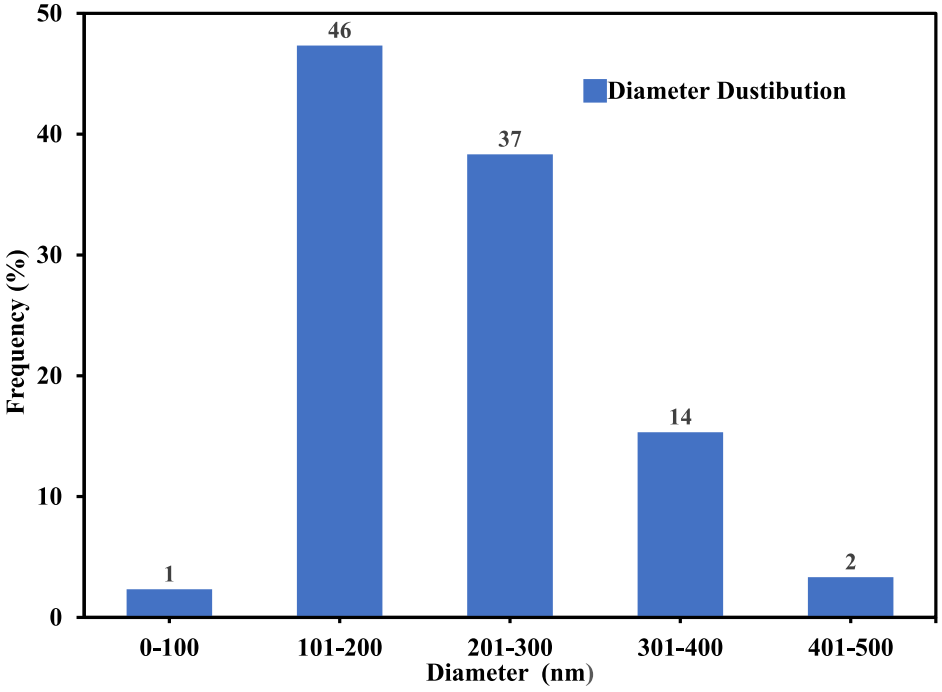


Fig. 4. The diameter distribution of the MoB nanofibre deposited in the modified bandage after 8 h.

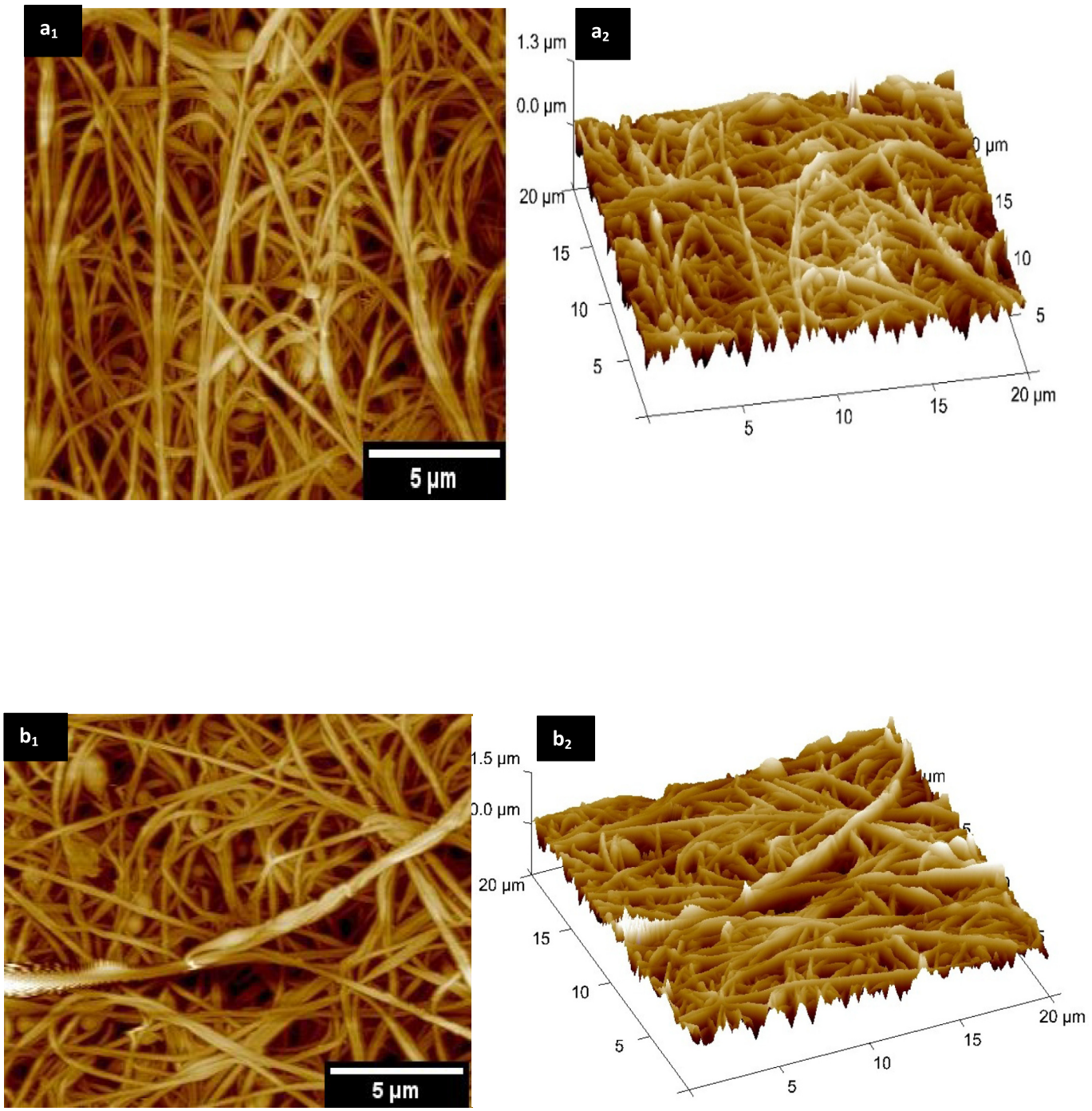


Fig. 5. (a_1) 2-Dimensional (2-D), (a_2) 3-dimensional (3-D) topography of the UcB and (b_1) 2-dimensional (2-D), (b_2) 3-dimensional (3-D) topography of the MoB.

nm in the MoB. This influence is an attribute of a well-textured surface, which can be helpful during the wound healing process, enabling enough area for cell attachment and proliferation for new tissue or cell formation. [64,65]. The texture can help trap moisture and maintain a suitable environment. Studies have also shown that water vapour is necessary for adequate wound dressing for normal skin [66]. The topographical analysis demonstrates that the cross-linked bandage provides several advantages over the uncross-linked bandage, owing to its enhanced roughness and surface texture area. These may include improved drug delivery capability, enhanced cell adhesion during wound healing, better moisture retention, and higher antimicrobial efficacy, making it a more effective solution for wound healing and infection control.

4.3. FTIR analysis of OEO(carvacrol and thymol), SAg, UcB, and MoB

Fig. 6 presents the ATR-FTIR spectra of the OEO, SAg, UcB, and MoB. A broad peak between 3100 cm^{-1} and 3600 cm^{-1} centred at 3386 cm^{-1}, is attributed to OH stretching vibrations predominantly common to most essential oils [67,68]. The peaks between 2859 cm^{-1}, 2969 cm^{-1}, and 2917 cm^{-1} can be ascribed to the symmetric and asymmetric -CH stretching vibration [69] OEO. The peaks centred at 1721 cm^{-1} are reportedly related to anhydride, while peaks at 1585 cm^{-1} and 1525 cm^{-1} are attributed to the C═C stretching peaks of aromatic rings, respectively [67,70]. The visible peaks at 1422 cm^{-1} are ascribed to CH_2 bending vibrations. The peaks 1361 cm^{-1} are characteristic of the main constituents of carvacrol and thymol, the main OEO constituent

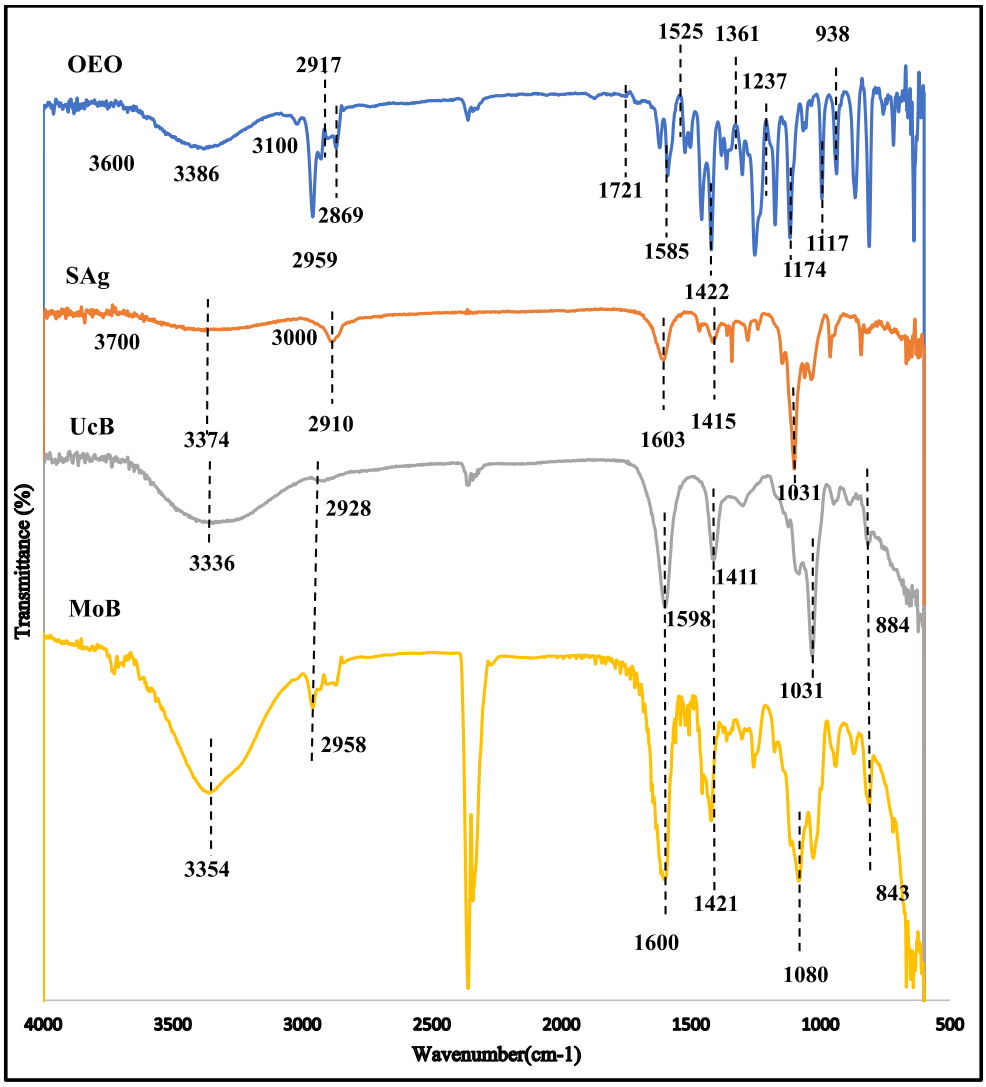


Fig. 6. Fourier transform infrared (FTIR) spectral analysis of OEO, SAg, UcB, and MoB.

responsible for the antibacterial effect. The stretching vibration peaks at 1237 cm^{-1}, 1174 $cm^{-1,}$ and 1117 cm^{-1} are attributed to C-C-O. The peaks at 936 cm^{-1} are related to the C—H bending of oregano oil [71,72].

The FTIR spectra of SAg have been recently reported by Orisawayi et al., [16]. With minor variations and shifts in peaks. The broad peaks cantered at 3374 of (between 3700 and 3000) are ascribed to OH stretching, peaks at 2910, 1603, and 1415 related to -CH_2 groups, symmetric and symmetric stretching of -COONa in Carboxylate Salt of sodium alginate [73].

The spectra of UcB and MoB are similar, with shifts in peaks resulting from cross-linking processes and the removal of PEO after soaking, washing, and drying MoB. Notably, the broad spectral range centred at 3336 cm^{-1} in UcB shifted to 3354 in MoB, which is predominantly attributed to intermolecular hydrogen bonding between the hydroxyl groups of alginates and the pure cellulose or regenerated polymer chains of the cotton bandage which may be similar to studies on confirmation of OH-stretching vibrations in this region as an indication of hydrogen bonding within polysaccharide systems [74]. The aromatic ring vibrations appear at 1598 cm^{-1} in UcB and shift to 1600 cm^{-1} in MoB. The displacement of bands is ascribed to different groups and interactions between the components. Initially, these displacements were attributed to the interaction between OEO and alginate and to changes resulting from crosslinking with calcium chloride. However, these same shifts could also reflect the interaction between alginate and cellulose in the cotton gauze. Since both interactions involve polar molecules, this possible displacement could be due to hydrogen bonding and other molecular interactions involving polar functional groups [75].

Furthermore, the peak at 1598 cm^{-1} shifted to 1600 cm^{-1} can also indicate the asymmetric and symmetric stretching of carboxylate groups (–COONa) in sodium alginate. Changes upon cross-linking with calcium chloride, due to substituting sodium ions with calcium ions, alter the alginate structure from sodium alginate to calcium alginate. [76] The initial peak at 936 cm^{-1} in OEO, related to C—H bending, disappears in UcB and MoB, potentially reappearing as 884 cm^{-1} in UcB and 843 cm^{-1} in MoB, due to the removal of PEO. The OEO appearing in the spectrum of OEO-SAG demonstrates the successful incorporation of OEO into MoB.

The FTIR spectra further provide more insights into the adhesion mechanism of alginate nanofibres to the cotton bandage. The molecular interactions between alginate and cotton the cellulose polymer chains present in the cotton bandage primarily govern this [77]. The broad peaks around the OH stretching band observed in UcB, and MoB cantered at 3354 cm^{-1} in MoB suggest strong intermolecular hydrogen bonding, a key interaction between alginate nanofibre and cellulose fibres in the cotton bandage. This interaction is like the findings of Yadav et al. (2021) [78] who studied bio-extract amalgamated alginate-cellulose nanofibres in three-dimensional sponges with

interpenetrating BioPU coatings for potential wound care applications. Their study highlighted the crucial role of hydrogen bonding in enhancing the adhesion and stability of alginate-cellulose nanofibre-based structures, further supporting the observed molecular interactions in this work.

Additionally, the shift in peaks from 1598 cm^{-1} in UcB to 1600 cm^{-1} in MoB could also be attributed to increased hydrogen bonding interactions between alginate and the cellulose polymer chains of the cotton bandage. However, these findings show that it could be related to both alginate and cellulose exhibiting strong molecular interactions, primarily through hydrogen bonding. This is supported by the literature on alginate-cellulose hydrogen bonding [79,80]. This favourable secondary interaction allows excellent adhesion between alginate nanofibres and the cotton bandage, as observed in our experiments. The experimental observations confirmed that the alginate nanofiber film deposition exhibited remarkable adhesion to the cotton bandage, further supporting the role of hydrogen bonding in this interaction. These FTIR findings confirm the structural modifications and intermolecular interactions observed might be responsible for the enhanced adhesion of the developed nanofibre on the cotton bandage.

4.4. TGA analysis of UcB and MoB

Previous studies have been able to carry out the thermal degradation of cotton gauze, and pristine alginate has been previously studied and reported extensively [81]. This current work focused on composite interactions. Fig. 7 shows the thermal degradation properties of the UcB and MoB. The uncross-linked samples (UcB) had a weight loss of approximately 50 to 79.91 °C at 4.6 wt% may be due to the evaporation of water or volatiles from the combination of the alginate and the oregano essential oil [82]. Degradation steps at onset 221 °C and 237 °C, at 9.7 wt% likely indicates alginate and oregano oil decomposition. The primary decomposition that occurs at around n and 358 °C at 31.354 wt % could be attributed to the breakdown of the alginate backbone or the presence of the PEO degradation present in the inelastic inclined bandage material, as the bandage may be made from cotton, which is related to the attribute behaviour of cellulose [83]. A smaller weight loss occurred at approximately 479 °C at 3.6 wt% may relate to the breakdown of final residual components in the combination of the matrix and burning of the residual components. The cross-linked bandage sample (MoB) also shows a similar weight loss at 32 °C and 70.4° at a higher weight loss of approximately 12.821 wt% similar to moisture or solvent entrapped within the matrix of the cross-linked essential oils embedded into the alginate or polymer matrix [84,85]. There is an enhanced thermal stability, as seen by less pronounced weight loss around 256 °C and 336 °C at 11 wt%. The additional degradation at 359 and 378 °C may be due to the cross-linked alginate matrix breakdown, and final degradation beyond 516.7 °C evident that there is additional degradation that may be attributed to additional bonds bond formation during cross-linking that could improve the formation of stability of the as the PEO has been removed after cross-linking, soaking, and drying the bandage similar to previous literatures [86,87]. The degradation stability is well structured for wound dressing applications [15]. The difference in the thermal and variation in the properties, which is in line with previous studies that cross-linked alginate with essential oils observed in the thermal properties of the MoB [88–90].

4.5. Antibacterial evaluation

Previous studies show that OEO is effective against MRSA and *L. monocytogenes* [39,91]. Similar behaviour was tailored to be used in our antimicrobial because of positive confirmation of the antimicrobial effect of OEO against these bacteria mentioned above. Modified bandages were exposed to bacterial lawns grown on agar for 24 h, and inhibitory zones were recorded against MRSA (Fig. 8) (Fig. 9) and *L. monocytogenes* (Fig. 10). Exposure to the single-layered bandage samples (single-sided or double-sided) resulted in smaller zones of inhibition compared to the 2-layer bandage, where the single-sided sample also had no observed antibacterial effect against *L. monocytogenes*. Our antibacterial assay results show inhibition zones of 10–15 mm against *Listeria monocytogenes* and Methicillin-resistant *Staphylococcus aureus* (MRSA) using the multilayered electrospun bandage (TL-BSS), compared to 6–8.5 mm reported by Lu et al. [15] for a similar electrospun alginate-oregano oil (OEO) composite. This suggests that our optimised nanofibre deposition, cross-linking technique, and multilayered structure enhance antibacterial efficacy. The improved performance may be attributed to structural differences, with 38–105 nm fibre diameters, whereas ours range from 100 to 200 nm. The larger diameter likely improves OEO encapsulation and sustained antimicrobial release in the fibre. It was also reported that an increase in nanofibre density

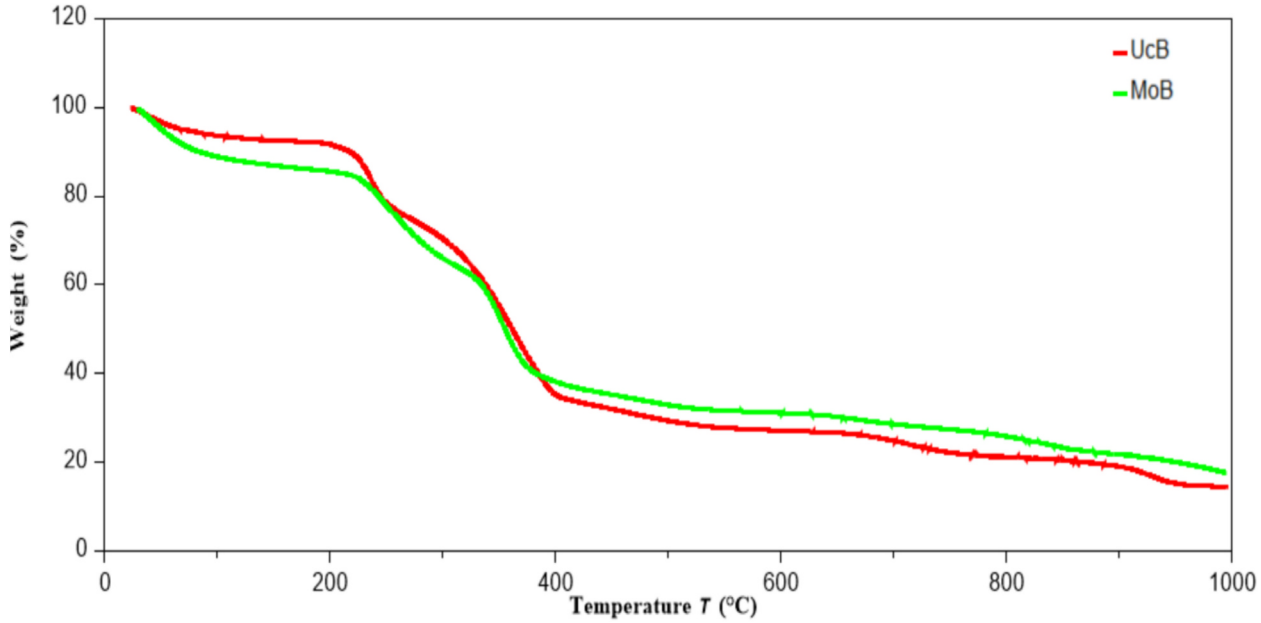


Fig. 7. TGA comparison of uncross-linked (UcB) and cross-linked (MoB) bandages.

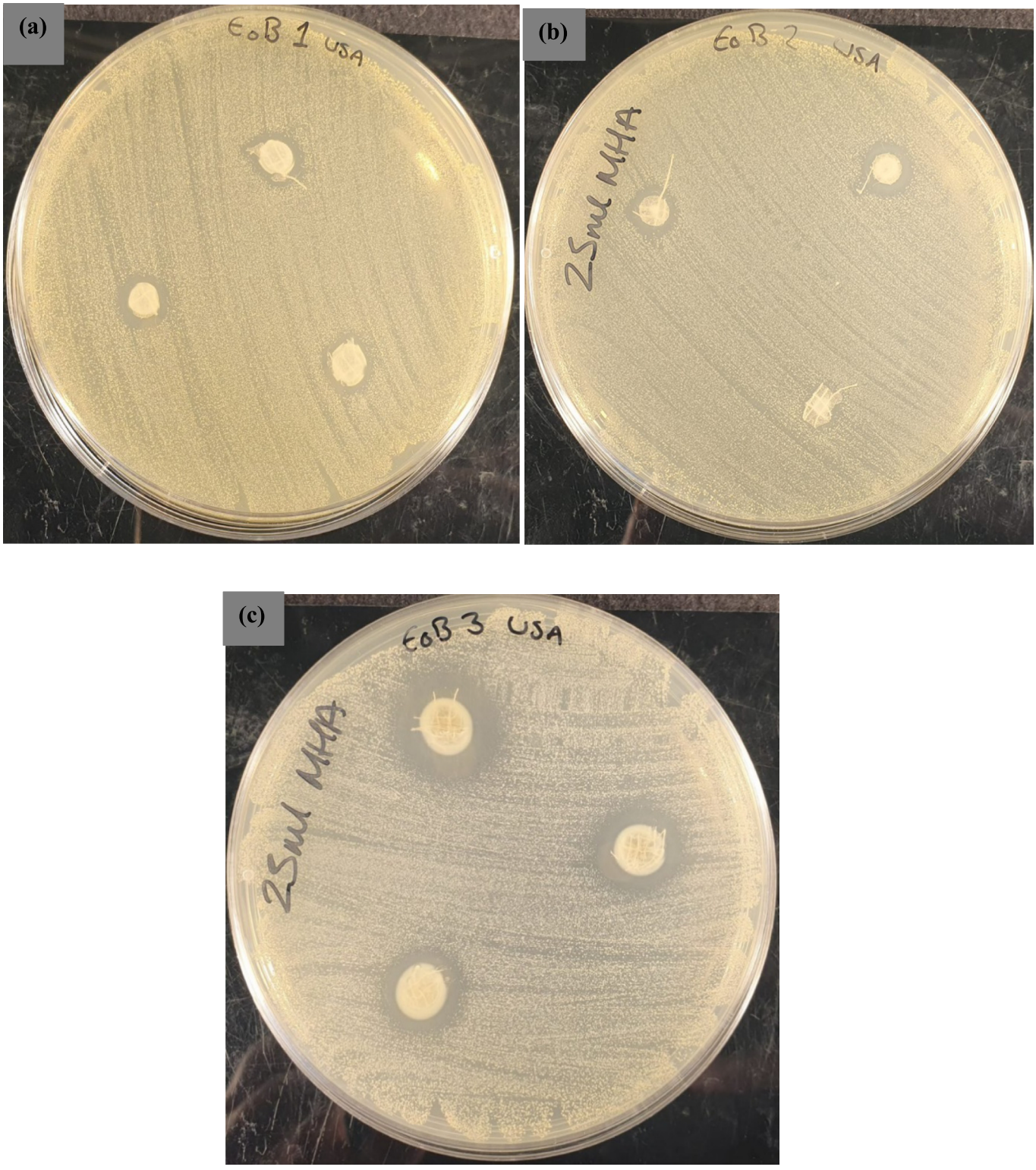


Fig. 8. Shows the antibacterial activity of bandages against MRSA, with SSS (a), BSS (b), and (c) TL-BSS.

could the matrix interactions contributing to effective bacterial inhibition [81]; this result could have made our multilayered electrospun bandage superior over its counterpart composited without a bandage. Bandage samples alone without incorporated alginate. These antibacterial assay results demonstrated that the Sag-OEO nanofibres, which were incorporated into the bandage, successfully added an antibacterial effect to the sample. Whilst the inhibitory effect was noticeably different for wound infection-causing bacteria (MRSA) compared to foodborne bacteria (*L. monocytogenes*), the results demonstrated that these have the potential to be used as both antimicrobial bandages/wound dressings and as antimicrobial food packaging. Parkale et al., [92] reported a smart cotton fabric as a potential next-generation dressing material. In their study, cotton was coated on a gauze bandage (CGB) with chitosan and ZnO nanoparticles. The resulting product was decorated with CGB by depositing Diclofenac sodium drug-loaded polycaprolactone biodegradable nanofibres. The CGB with chitosan coating and ZnO

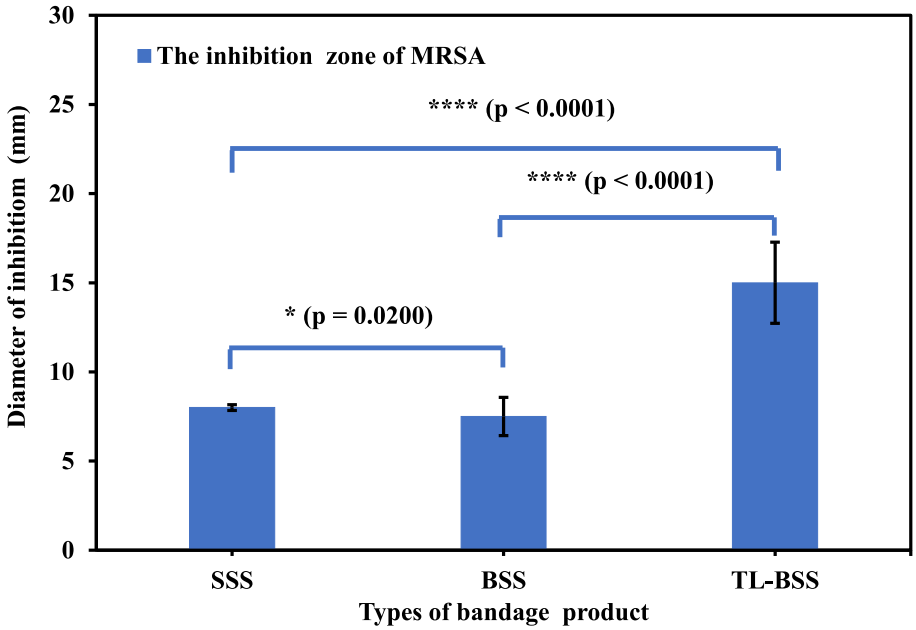


Fig. 9. The diameter of the inhibitory zones following modified bandage exposure to MRSA. Error bars represent the standard error of the mean for $n = 3$ (ordinary one way- ANOVA and Tukey's multiple comparison test: $p > 0.05$ NS not significant, $p \leq 0.05$ * significant, $0.01 \leq p < 0.05$ * moderately significant, $0.001 \leq p < 0.01$ ** very significant, $p < 0.001$ **** highly significant.)

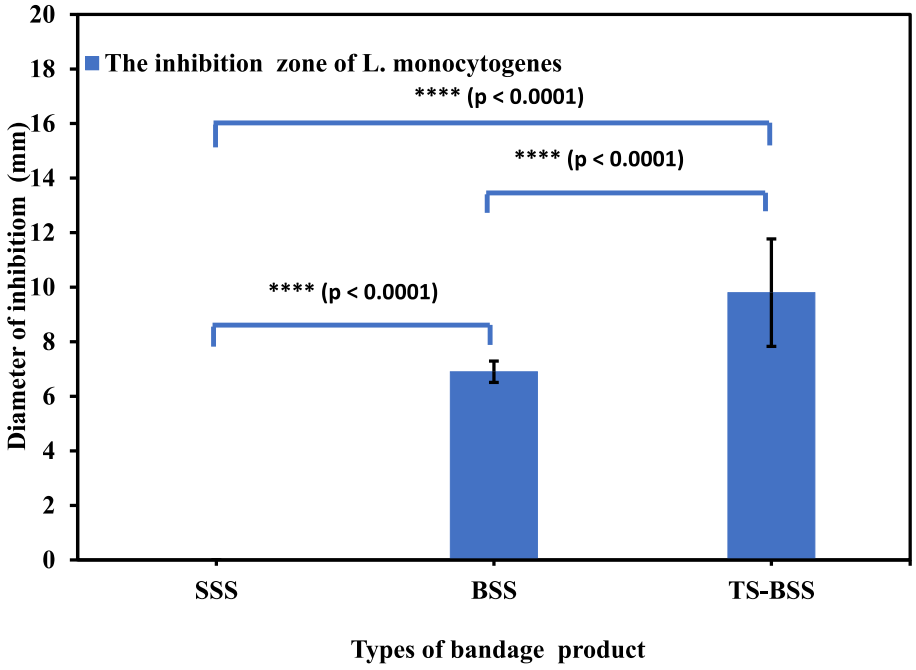


Fig. 10. The diameter of the inhibitory zones following modified bandage exposure to *L. monocytogenes*. Error bars represent the standard error of the mean for $n = 3$. (Ordinary one way-ANOVA and Tukey's multiple comparison test: $p > 0.05$ NS not significant, $p \leq 0.05$ * significant, $0.01 \leq p < 0.05$ * moderately significant, $0.001 \leq p < 0.01$ ** very significant, $p < 0.001$ **** highly significant.)

demonstrated sound antibacterial effects and UV screening properties [92]. In comparison with a previous study, Parkdale et al. [92] in our current study, the carrier material is alginate, which is renewable and derived from a natural source, unlike Polycaprolactone (PCL), a synthetic polymer and Chitosan used in the previous study are more expensive than alginate.

From the choice of medicinal perspectives, the purely natural and renewable oregano essential oil has a broad-spectrum antibacterial effect. ZnO nanoparticles are known to be more toxic and may result in environmental pollution risks; hence, the use of ZnO nanoparticles may not be suitable for medical bandage application [93].

4.6. Statistical analysis of antibacterial activity of electrospun bandage configurations against MRSA and L. monocytogenes

The evaluation of the antibacterial activity of the modified electrospun bandage samples (SSS, BSS, and TL-BSS) against MRSA and L. *monocytogenes* was also presented in Figure (Figs. 9 and 10). The analysis

of variance (ANOVA) presented a F-statistic value of 2857 and R^2 value of 0.9992 close to 1 an excellent fit which indicates that the model is 99.92 % of the total variance, which could be attributed to extremely strong effect of treatment on bacterial inhibition.

The Statistical Significance of Bandage Configurations Against MRSA obtained from the comparison between SSS and BSS was statistically significant ($p = 0.0200$), suggesting that electrospinning on both sides of the bandage improves antibacterial performance. The comparisons SSS vs. TL-BSS and BSS vs. TL-BSS ($p < 0.0001$) confirmed that multilayered structures significantly enhance bacterial inhibition, due to increased nanofiber density and surface interaction with bacteria. This may be due to the layer stacking contributes that could contribute to the antibacterial effectiveness of TL-BSS against MRSA of the alginate oregano oils nanofibres [15].

Furthermore, all statistical Significance of the bandage configurations against the *L. monocytogenes* bacterial comparisons, including SSS vs. BSS, SSS vs. TL-BSS, and BSS vs. TL-BSS, were highly significant ($p < 0.0001$). This confirms that a multilayered structure (TL-BSS) leads to more significant bacterial inhibition against *L. monocytogenes*, further reinforcing the hypothesis that increased nanofiber deposition enhances the antibacterial activity which has been previously reported [94].

These results suggest that the comparison of the bandage configurations on the antibacterial activity shows that the TL-BSS configuration consistently exhibited the most significant inhibition zones for both MRSA and *L. monocytogenes*, indicating an enhancement in the antibacterial activity compared to single-sided (SSS) and both-sided spun (BSS) bandages. Conversely, the SSS configuration displayed the most minor inhibition zones across both bacterial strains, suggesting that limited nanofiber deposition may reduce antibacterial efficacy [95].

The statistical analysis confirmed that the nanofiber deposition configuration of alginate-oregano oil nanofibres significantly influences antibacterial properties, thereby improving the effectiveness of the electrospun bandages. The TL-BSS bandage configuration was the most effective in inhibiting MRSA, while it also considerably inhibited *L. monocytogenes* but to a lesser extent. From a hypothesis testing perspective, the results indicate that the null hypothesis (H_0) was rejected, as no instances of non-significance (NS; $p > 0.05$) were observed. The statistical analysis provided sufficient evidence to confirm significant differences among the sample configurations. This led to the acceptance of the alternative hypothesis (H_1), confirming that different electrospinning configurations significantly impact antibacterial performance. These findings contribute valuable insights into developing advanced antimicrobial wound dressing materials with potential applications in clinical infection control and wound management.

5. Limitations and future perspectives

The findings from this study are promising; however, certain limitations should be acknowledged to provide a comprehensive evaluation of the developed electrospun Sag-OEO nanofibre bandage and to guide future research. The optimisation of the electrospinning process parameters, such as solution concentration, applied voltage, and humidity control, was not extensively explored, addressing this could further enhance the uniformity of deposition. There was no mechanical test, such as tensile strength, flexibility, or durability test. Another key limitation is that the study was limited to in vitro, as no in vivo validation was conducted, as antibacterial efficacy and wound healing potential could be validated through both in vitro and in vivo; therefore incorporates both time-kill kinetics. In our future study we would focus on addressing these aspects by conducting mechanical characterisation and conduct an in depth optimising on both the solution and the electrospinning process parameters, the release characteristics of oregano essential oil (OEO) from the nanofibre matrix were not fully explored, necessitating further studies to evaluate its sustained antimicrobial efficacy. Furthermore, our ongoing work is to address the in vivo studies to confirm the clinical application, and we will explore the efficacy of the Sag-OEO nanofibre bandage against a broader range of clinically relevant bacteria, including Gram-negative bacteria such as *Pseudomonas aeruginosa* and *Escherichia coli*, which are known to complicate wound infections. Addressing these limitations will enhance the structural stability, bioactivity, and the potential of the Sag-OEO nanofibre bandage to find its antimicrobial applications.

6. Conclusion

This study marks a significant milestone for potential wound care applications, as we have successfully developed an effective antibacterial nanocomposite. By combining alginate and oregano essential oil (OEO) and carefully depositing nanofibres on a woven cotton gauze bandage substrate. Our study demonstrated a well-optimised electrospinning process that ensured consistent nanofibre formation, with progressive deposition observed over several hours. The resulting nanofibres ranged in diameter from 100 to 300 nm, significantly enhancing the surface area for controlled drug release and microbial interaction.

The cross-linking with calcium chloride has stabilised the nanofibrous structure, as evidenced by multiple characterisation techniques. Thermogravimetric Analysis (TGA) showed that cross-linked bandages had improved thermal stability compared to uncross-linked ones, with less weight loss at higher temperatures, indicating better structural integrity. The (FTIR) analysis confirmed the presence of key functional groups from alginate and OEO, with peak shifts from 1598 cm^{-1} to 1600 cm^{-1}, suggesting intermolecular interactions responsible for improved adhesion to the cotton bandage. Morphological and topographical analyses further validated the nanofibre formation. Scanning Electron Microscopy (SEM) revealed the morphology of the successful nanofibre deposited on the bandage surface, with fibres becoming more homogeneous and densely packed over time, forming a coherent network after cross-linking. Our analysis using Atomic Force Microscopy (AFM) also confirms that surface roughness ranges from 149.5 nm in uncross-linked samples to 176.5 nm in cross-linked samples, which is beneficial for enhancing cell attachment and proliferation, crucial for effective wound healing. The antibacterial evaluation revealed significant inhibitory activity against Methicillin-resistant *Staphylococcus aureus* (MRSA) and *Listeria monocytogenes*, demonstrating the bioactive potential of the electrospun bandage. The TL-BSS configuration exhibited the most significant inhibition zones (15 mm for MRSA and 10 mm for *L. monocytogenes*), reinforcing the hypothesis that increased nanofibre density enhances antibacterial properties. Statistical analysis (One-Way ANOVA and Tukey's multiple comparison test) confirmed significant differences ($p < 0.0001$) among bandage configurations, leading to the rejection of the null hypothesis (H_0) and confirming that nanofibre deposition significantly influences antibacterial effectiveness. These results validate the effectiveness of our nanocomposite and highlight its superior antimicrobial properties, which could be a game-changing solution for affordable medical care for millions across Africa and Asia.

CRediT authorship contribution statement

Abimbola Oluwatayo Orisawayi: Writing – review & editing, Writing – original draft, Validation, Software, Project administration, Methodology, Investigation, Funding acquisition, Formal analysis, Conceptualization. **Hao Lu:** Writing – review & editing, Writing – original draft, Visualization, Software, Project administration, Methodology, Investigation, Funding acquisition, Formal analysis, Conceptualization. **Ishrat Jahan Badruddin:** Writing – review & editing. **Prabhuraj D. Venkatraman:** Writing – review & editing, Validation, Supervision, Resources, Project administration, Investigation, Funding acquisition, Formal analysis, Conceptualization. **Nicole S. Britten:** Writing – review & editing, Visualization, Validation, Supervision, Resources, Project administration, Methodology, Investigation, Funding acquisition, Formal analysis, Conceptualization. **Jonathan A. Butler:**

Writing – review & editing, Visualization, Validation, Supervision, Resources, Project administration, Methodology, Investigation, Funding acquisition, Formal analysis, Conceptualization. **Krzysztof Koziol:** Writing – review & editing, Supervision, Resources. **Sameer S. Rahatekar:** Writing – review & editing, Visualization, Validation, Supervision, Resources, Project administration, Methodology, Investigation, Funding acquisition, Formal analysis, Conceptualization.

Funding

The authors would like to acknowledge the Biomass Biorefinery Network (BBNet), the Biotechnology and Biological Sciences Research Council (BBSRC) for their partial funding and the Petroleum Technology Development Fund (PTDF) for sponsorship and scholarship support Award Number: PTDF/ED/OSS/PHD/AOO/1844/2020PHD152.

Declaration of competing interest

The authors declare that they have no known competing commercial interests or personal relationships that could have appeared to influence the work reported in this paper.

Acknowledgements

The authors would like to thank the technicians Jim Hurley, Diane Johnson, Kris Bramley, and Christine Kimpton for their assistance with SEM and AFM analysis, Dr. David Ayre for his training on TGA, and all the staff of the Composites and Advanced Materials Centre at Cranfield University for their invaluable technical support, partial funding and encouragement during the experimental work.

Data availability

Data will be made available on request.

References

[1] M. Farahani, A. Shafiee, Wound healing: from passive to smart dressings, Adv. Healthc. Mater. 10 (2021) 1–32, https://doi.org/10.1002/adhm.202100477.
[2] X. Deng, M. Gould, M.A. Ali, A review of current advancements for wound healing: biomaterial applications and medical devices, J. Biomed. Mater. Res. B Appl. Biomater. 110 (2022) 2542–2573, https://doi.org/10.1002/jbm.b.35086.
[3] N. Kim, H. Lee, G. Han, M. Kang, S. Park, D.E. Kim, M. Lee, M. Kim, Y. Na, S. Oh, S. Bang, T. Jang, H. Kim, J. Park, S.R. Shin, H. Jung, 3D-printed functional hydrogel by DNA-induced biomineralization for accelerated diabetic wound healing, Adv. Sci. 10 (2023), https://doi.org/10.1002/advs.202300816.
[4] E. Mavrokefalou, P.K. Monou, D. Tzetzis, N. Bouropoulos, I.S. Vizirianakis, D. G. Fatouros, Preparation and in vitro evaluation of electrospun sodium alginate fiber films for wound healing applications, J Drug Deliv Sci Technol 81 (2023) 1–9, https://doi.org/10.1016/j.jddst.2023.104298.
[5] T.G. Sahana, P.D. Rekha, Biopolymers: applications in wound healing and skin tissue engineering, Mol. Biol. Rep. 45 (2018) 2857–2867, https://doi.org/10.1007/s11033-018-4296-3.
[6] T. Huang, Z. Sun, D.E. Heath, N. O'Brien-Simpson, A.J. O'Connor, 3D printed and smart alginate wound dressings with pH-responsive drug and nanoparticle release, Chem. Eng. J. 492 (2024) 1–14, https://doi.org/10.1016/j.cej.2024.152117.
[7] A. Ravindran Girija, V. Palaninathan, X. Strudwick, S. Balasubramanian, S. Dasappan Nair, A.J. Cowin, Collagen-functionalized electrospun smooth and porous polymeric scaffolds for the development of human skin-equivalent, RSC Adv. 10 (2020) 26594–26603, https://doi.org/10.1039/D0RA04648E.
[8] A. Soto-Quintero, P. González-Alva, A. Covelo, M.A. Hernández, Study of the in vitro degradation and characterization of the <scp>HaCat</scp> keratinocytes adherence on electrospun scaffolds based polyvinyl alcohol/sodium alginate, J. Appl. Polym. Sci. 139 (2022) 2–14, https://doi.org/10.1002/app.52775.
[9] A. Verma, A. Zanoletti, K.Y. Kareem, B. Adelodun, P. Kumar, F.O. Ajibade, L.F. O. Silva, A.J. Phillips, T. Kartheeswaran, E. Bontempi, A. Dwivedi, Skin protection from solar ultraviolet radiation using natural compounds: a review, Environ. Chem. Lett. 22 (2024) 273–295, https://doi.org/10.1007/s10311-023-01649-4.
[10] M. Venus, J. Waterman, I. McNab, Basic physiology of the skin, Surgery (Oxford) 28 (2010) 469–472, https://doi.org/10.1016/j.mpsur.2010.07.011.
[11] M.R. Zare, M. Khorram, S. Barzegar, F. Asadian, Z. Zareshahrabadi, M.J. Saharkhiz, S. Ahadian, K. Zomorodian, Antimicrobial core–shell electrospun nanofibers containing Ajwain essential oil for accelerating infected wound healing, Int. J. Pharm. 603 (2021) 1–15, https://doi.org/10.1016/j.ijpharm.2021.120698.
[12] H. Alvandi, M. Jaymand, M. Eskandari, F. Aghaz, L. Hosseinzadeh, M. Heydari, E. Arkan, A sandwich electrospun nanofibers/Tragacanth hydrogel composite containing Aloe vera extract and silver sulfadiazine as a wound dressing, Polym. Bull. 80 (2023) 11235–11248, https://doi.org/10.1007/s00289-022-04603-6.
[13] A. Sharma, A. Mittal, V. Puri, P. Kumar, I. Singh, Curcumin-loaded, alginate–gelatin composite fibers for wound healing applications, 3 Biotech 10 (2020) 464, https://doi.org/10.1007/s13205-020-02453-5.
[14] S.A. Elghobashy, A.B. Abeer Mohammed, A.A. Tayel, F.A. Alshubaily, A. Abdella, Thyme/garlic essential oils loaded chitosan–alginate nanocomposite: characterization and antibacterial activities, E-Polymers 22 (2022) 997–1006, https://doi.org/10.1515/epoly-2022-0090.
[15] H. Lu, J.A. Butler, N.S. Britten, P.D. Venkatraman, S.S. Rahatekar, Natural antimicrobial nano composite fibres manufactured from a combination of alginate and oregano essential oil, Nanomaterials 11 (2021) 1–16, https://doi.org/10.3390/NANO11082062.
[16] A.O. Orisawayi, K. Koziol, S. Hao, S. Tiwari, S.S. Rahatekar, Development of hybrid electrospun alginate-pulverized moringa composites, RSC Adv. 14 (2024) 8502–8512, https://doi.org/10.1039/D4RA00162A.
[17] F.O. Adetuyi, E.S. Akintimehin, K.O. Karigidi, A.O. Orisawayi, Safety evaluation of fermented and nonfermented Moringa oleifera seeds in healthy albino rats: biochemical, haematological, and histological studies, Int J Food Sci 2025 (2025) 1–12, https://doi.org/10.1155/ijfo/2694100.
[18] V.M. Wheatley, J. Spink, Defining the public health threat of dietary supplement fraud, Compr. Rev. Food Sci. Food Saf. 12 (2013) 599–613, https://doi.org/10.1111/1541-4337.12033.
[19] Z. Chen, J. Song, Y. Xia, Y. Jiang, L.L. Murillo, O. Tsigkou, T. Wang, Y. Li, High strength and strain alginate fibers by a novel wheel spinning technique for knitting stretchable and biocompatible wound-care materials, Mater. Sci. Eng. C 127 (2021) 1–11, https://doi.org/10.1016/j.msec.2021.112204.
[20] M.G. Nur, M. Rahman, T.M. Dip, M.H. Hossain, N.B. Hossain, S. Baratchi, R. Padhye, S. Houshyar, Recent advances in bioactive wound dressings, Wound Repair Regen. 33 (2025) 1–29, https://doi.org/10.1111/wrr.13233.
[21] M.C.F. Smith, C. Huins, M. Bhutta, Surgical treatment of chronic ear disease in remote or resource-constrained environments, J. Laryngol. Otol. 133 (2019) 49–58, https://doi.org/10.1017/S0022215118002165.
[22] R. Bashir, T. Ali, S.N. Raza, N.A. Khan, Overview of nanofibres as ideal drug delivery systems for pharmaceutical and medicinal applications, Bionanoscience 15 (2025) 1–15, https://doi.org/10.1007/s12668-024-01640-5.
[23] F. Xie, Alginate-based nanocomposites for food preservation: recent progress showcasing heightened material properties and functionalities, Advanced Nanocomposites 1 (2024) 248–274, https://doi.org/10.1016/j.adna.2024.07.002.
[24] Y. Tang, X. Lan, C. Liang, Z. Zhong, R. Xie, Y. Zhou, X. Miao, H. Wang, W. Wang, Honey loaded alginate/PVA nanofibrous membrane as potential bioactive wound dressing, Carbohydr. Polym. 219 (2019) 113–120, https://doi.org/10.1016/j.carbpol.2019.05.004.
[25] J. Li, H. Lin, J. Li, Y. Wang, Engineered lubricative lecithin-based electrospun nanofibers for the prevention of postoperative abdominal adhesion, Pharmaceutics 16 (2024) 1–15, https://doi.org/10.3390/pharmaceutics16121562.
[26] K.C. Gupta, A. Haider, Y. Choi, I. Kang, Nanofibrous scaffolds in biomedical applications, Biomater Res 18 (2014) 1–11, https://doi.org/10.1186/2055-7124-18-5.
[27] I.O. Oladele, S.O. Adelani, A.S. Taiwo, I.M. Akinbamiyorin, O.F. Olanrewaju, A. O. Orisawayi, Polymer-based nanocomposites for supercapacitor applications: a review on principles, production and products, RSC Adv. 15 (2025) 7509–7534, https://doi.org/10.1039/D4RA08601E.
[28] J. Wang, C. You, Y. Xu, T. Xie, Y. Wang, Research advances in electrospun nanofiber membranes for non-invasive medical applications, Micromachines (Basel) 15 (2024) 1–32, https://doi.org/10.3390/mi15101226.
[29] K. Chen, H. Hu, Y. Zeng, H. Pan, S. Wang, Y. Zhang, L. Shi, G. Tan, W. Pan, H. Liu, Recent advances in electrospun nanofibers for wound dressing, Eur. Polym. J. 178 (2022) 1–14, https://doi.org/10.1016/j.eurpolymj.2022.111490.
[30] A. Abedi, M. Hasanzadeh, L. Tayebi, Conductive nanofibrous chitosan/PEDOT:PSS tissue engineering scaffolds, Mater. Chem. Phys. 237 (2019) 1–8, https://doi.org/10.1016/j.matchemphys.2019.121882.
[31] E. Lamei, M. Hasanzadeh, Concurrent electrospinning of microporous metal-organic framework-laden casein/PVA nanofibrous composites for potential antibacterial wound dressing applications, International Journal of Polymeric Materials and Polymeric Biomaterials 73 (2024) 637–645, https://doi.org/10.1080/00914037.2023.2191199.
[32] L. Asadi, J. Mokhtari, M. Abbasi, An alginate–PHMB–AgNPs based wound dressing polyamide nanocomposite with improved antibacterial and hemostatic properties, J. Mater. Sci. Mater. Med. 32 (2021) 1–11, https://doi.org/10.1007/s10856-020-06484-5.
[33] E. Lamei, M. Hasanzadeh, Fabrication of chitosan nanofibrous scaffolds based on tannic acid and metal-organic frameworks for hemostatic wound dressing applications, Int. J. Biol. Macromol. 208 (2022) 409–420, https://doi.org/10.1016/j.ijbiomac.2022.03.117.
[34] X. Zhao, J. Gao, X. Hu, H. Guo, F. Wang, Y. Qiao, L. Wang, Collagen/polyethylene oxide nanofibrous membranes with improved hemostasis and cytocompatibility for wound dressing, Appl. Sci. 8 (2018) 1–14, https://doi.org/10.3390/app8081226.
[35] P.M. Tyubaeva, I.A. Varyan, E.D. Nikolskaya, N.G. Yabbarov, M.V. Chirkina, M. B. Sokol, M.R. Mollaeva, L.V. Yurina, A.D. Vasilyeva, M.A. Rosenfeld, S. I. Obydennyi, I.A. Chabin, A.A. Popov, Electrospinning of biomimetic materials with fibrinogen for effective early-stage wound healing, Int. J. Biol. Macromol. 260 (2024) 1–12, https://doi.org/10.1016/j.ijbiomac.2024.129514.

[36] M.E. Talukder, K.M.F. Hasan, J. Wang, J. Yao, C. Li, H. Song, Novel fibrin functionalized multilayered electrospun nanofiber membrane for burn wound treatment, J. Mater. Sci. 56 (2021) 12814–12834, https://doi.org/10.1007/s10853-021-06123-6.
[37] M. Wang, C. Huang, Y. Chen, Y. Ji, D.-G. Yu, S.W.A. Bligh, Medicated tri-layer fibers based on cellulose acetate and polyvinylpyrrolidone for enhanced antibacterial and wound healing properties, Carbohydr. Polym. 348 (2025) 1–11, https://doi.org/10.1016/j.carbpol.2024.122856.
[38] X. Xie, D. Li, Y. Chen, Y. Shen, F. Yu, W. Wang, Z. Yuan, Y. Morsi, J. Wu, X. Mo, Conjugate electrospun 3D gelatin nanofiber sponge for rapid hemostasis, Adv. Healthc. Mater. 10 (2021) 1–13, https://doi.org/10.1002/adhm.202100918.
[39] R. Cabrera-Contreras, R. Morelos-Ramírez, J.P. Quiróz-Ríos, D. Muñoz-Quiróz, Antibacterial effects of oregano essential oil (OEO) and its potential applications, Microbiol Res J Int (2020) 19–25, https://doi.org/10.9734/mrji/2020/v30i430209.
[40] M. Alboofetileh, M. Rezaei, H. Hosseini, M. Abdollahi, Antimicrobial activity of alginate/clay nanocomposite films enriched with essential oils against three common foodborne pathogens, Food Control 36 (2014) 1–7, https://doi.org/10.1016/j.foodcont.2013.07.037.
[41] C. Peng, Q. Wang, W. Xu, X. Wang, Q. Zheng, X. Liang, X. Dong, F. Li, L. Peng, A bifunctional endolytic alginate lyase with two different lyase catalytic domains from Vibrio sp. H204, Front Microbiol 15 (2024) 1–14, https://doi.org/10.3389/fmicb.2024.1509599.
[42] I. Partheniadis, G. Stathakis, D. Tsalavouti, J. Heinämäki, I. Nikolakakis, Essential oil—loaded nanofibers for pharmaceutical and biomedical applications: a systematic mini-review, Pharmaceutics 14 (2022) 1–24, https://doi.org/10.3390/pharmaceutics14091799.
[43] S. Jafari, A. Hematian Sourki, S. Pashangeh, Emulsion electrospinning of lemongrass essential oil-loaded Ferula haussknechtii gum/polyethylene oxide as bioactive coating, Food Hydrocolloids for Health 7 (2025) 1–13, https://doi.org/10.1016/j.fhfh.2025.100195.
[44] S.S. Shetty, D. Khurana, A. Suresh, P. Somu, A.K. Singh, B.N. Singh, Advancement in development of antimicrobial multilayered porous-fibrous biopolymeric scaffold for wound healing application, Int. J. Polym. Mater. Polym. Biomater. (2025) 1–21, https://doi.org/10.1080/00914037.2024.2443792.
[45] A. Robu, M.G.A. Kaya, A. Antoniac, D.A. Kaya, A.E. Coman, M.-M. Marin, R. Ciocoiu, R.R. Constantinescu, I. Antoniac, The influence of basil and cinnamon essential oils on bioactive sponge composites of collagen reinforced with hydroxyapatite, Materials 18 (2025) 1–23, https://doi.org/10.3390/ma18030626.
[46] M.G. Nur, M. Rahman, T.M. Dip, M.H. Hossain, N.B. Hossain, S. Baratchi, R. Padhye, S. Houshyar, Recent advances in bioactive wound dressings, Wound Repair Regen. 33 (2025) 1–29, https://doi.org/10.1111/wrr.13233.
[47] Y. Premjit, S. Pandhi, A. Kumar, D.C. Rai, R.K. Duary, D.K. Mahato, Current trends in flavor encapsulation: a comprehensive review of emerging encapsulation techniques, flavour release, and mathematical modelling, Food Res. Int. 151 (2022) 1–15, https://doi.org/10.1016/j.foodres.2021.110879.
[48] I.B. Basumatary, L.S. Devi, A. Mukherjee, S. Kumar, Nanoemulsion in sustainable food packaging and preservation, in: Sustainable Materials for Food Packaging and Preservation, Elsevier, 2025, pp. 317–331, https://doi.org/10.1016/B978-0-443-13567-5.00015-0.
[49] L. Khullar, K. Harjai, S. Chhibber, Therapeutic and pro-healing potential of advanced wound dressings loaded with bioactive agents, Future Microbiol. 18 (2023) 43–63, https://doi.org/10.2217/fmb-2022-0162.
[50] I. dos Santos Paglione, M.V. Galindo, J.A.S. de Medeiros, F. Yamashita, I.D. Alvim, C.R. Ferreira Grosso, L.S. Sakanaka, M.A. Shirai, Comparative study of the properties of soy protein concentrate films containing free and encapsulated oregano essential oil, Food Packag Shelf Life 22 (2019) 2–8, https://doi.org/10.1016/j.fpsl.2019.100419.
[51] C. Patiño Vidal, G. López, I. Quinchiguango, C. Muñoz-Shugulí, Valorization of faba bean (*Vicia faba*) pods for the development of antibacterial starch-based films, ACS Food Science & Technology (2025) 1–9, https://doi.org/10.1021/acsfoodscitech.4c00768.
[52] Y. Yin, C. Guo, Q. Mu, W. Li, H. Yang, Y. He, Dual-sensing nano-yarns for real-time pH and temperature monitoring in smart textiles, Chem. Eng. J. 500 (2024) 1–11, https://doi.org/10.1016/j.cej.2024.157115.
[53] D. Sanders, A. Grunden, R.R. Dunn, A review of clothing microbiology: the history of clothing and the role of microbes in textiles, Biol. Lett. 17 (2021) 1–13, https://doi.org/10.1098/rsbl.2020.0700.
[54] S. Rajendran, S.C. Anand, Developments in medical textiles, Text. Prog. 32 (2002) 1–42, https://doi.org/10.1080/00405160208688956.
[55] S.M. Hossaeini Marashi, S.M.R. Noori, M. Hashemi, M. Raeisi, S.M.A. Noori, Electrospinning of nanofibers incorporated with essential oils: applications in food, Curr. Pharm. Biotechnol. 24 (2023) 1881–1897, https://doi.org/10.2174/1389201024666230407094527.
[56] E. Mele, Electrospinning of essential oils, Polymers (Basel) 12 (2020) 1–16, https://doi.org/10.3390/polym12040908.
[57] M. Rafiq, T. Hussain, S. Abid, A. Nazir, R. Masood, Development of sodium alginate/PVA antibacterial nanofibers by the incorporation of essential oils, Mater Res Express 5 (2018) 1–15, https://doi.org/10.1088/2053-1591/aab0b4.
[58] G. El Fawal, M.M. Abu-Serie, Bioactive properties of nanofibers based on poly (vinylidene fluoride) loaded with oregano essential oil: fabrication, characterization and biological evaluation, J Drug Deliv Sci Technol 69 (2022) 1–11, https://doi.org/10.1016/j.jddst.2022.103133.
[59] H. Liu, Y. Bai, C. Huang, Y. Wang, Y. Ji, Y. Du, L. Xu, D.-G. Yu, S.W.A. Bligh, Recent progress of electrospun herbal medicine nanofibers, Biomolecules 13 (2023) 1–50, https://doi.org/10.3390/biom13010184.
[60] S. Hedayati, M. Tarahi, A. Iraji, M.H. Hashempur, Recent developments in the encapsulation of lavender essential oil, Adv. Colloid Interface Sci. 331 (2024) 1–18, https://doi.org/10.1016/j.cis.2024.103229.
[61] C. Shi, A. Zhou, D. Fang, T. Lu, J. Wang, Y. Song, L. Lyu, W. Wu, C. Huang, W. Li, Oregano essential oil/β-cyclodextrin inclusion compound polylactic acid/polycaprolactone electrospun nanofibers for active food packaging, Chem. Eng. J. 445 (2022) 1–13, https://doi.org/10.1016/j.cej.2022.136746.
[62] B. Suganya Bharathi, T. Stalin, Cerium oxide and peppermint oil loaded polyethylene oxide/graphene oxide electrospun nanofibrous mats as antibacterial wound dressings, Mater Today Commun 21 (2019) 1–11, https://doi.org/10.1016/j.mtcomm.2019.100664.
[63] K. Nathani, M. Damani, S. Mangrulkar, S. Sawarkar, Polymeric nanofibers derived therapeutic approach for skeletal muscle regeneration: the promising future of muscle repair, J Drug Deliv Sci Technol 94 (2024) 1–25, https://doi.org/10.1016/j.jddst.2024.105503.
[64] O. Bjorgvinsdottir, S.J. Ferguson, B.S. Snorradottir, T. Gudjonsson, K. Wuertz-Kozak, The influence of physical and spatial substrate characteristics on endothelial cells, Mater Today Bio 26 (2024) 1–16, https://doi.org/10.1016/j.mtbio.2024.101060.
[65] N. Mansouri, SamiraBagheri, The influence of topography on tissue engineering perspective, Mater. Sci. Eng. C 61 (2016) 906–921, https://doi.org/10.1016/j.msec.2015.12.094.
[66] M. Najafiasl, S. Osfouri, S. Zaeri, Evaluation of physicochemical properties, release kinetics, and in vitro/in vivo wound healing activity of the electrospun nanofibres loaded with the natural antioxidant oil from Pistacia atlantica, J Drug Deliv Sci Technol 84 (2023) 1–11, https://doi.org/10.1016/j.jddst.2023.104512.
[67] J. Wang, C. Chen, J. Xie, Loading oregano essential oil into microporous starch to develop starch/polyvinyl alcohol slow-release film towards sustainable active packaging for sea bass (Lateolabrax japonicus), Ind. Crop. Prod. 188 (2022) 1–13, https://doi.org/10.1016/j.indcrop.2022.115679.
[68] M. Mehran, S. Masoum, M. Memarzadeh, Microencapsulation of Mentha spicata essential oil by spray drying: optimization, characterization, release kinetics of essential oil from microcapsules in food models, Ind Crops Prod 154 (2020) 1–8, https://doi.org/10.1016/j.indcrop.2020.112694.
[69] R. Hernández-Nava, A. López-Malo, E. Palou, N. Ramírez-Corona, M.T. Jiménez-Munguía, Encapsulation of oregano essential oil (Origanum vulgare) by complex coacervation between gelatin and chia mucilage and its properties after spray drying, Food Hydrocoll. 109 (2020) 1–8, https://doi.org/10.1016/j.foodhyd.2020.106077.
[70] P. Sharma, A. Ahuja, A.M. Dilsad Izrayeel, P. Samyn, V.K. Rastogi, Physicochemical and thermal characterization of poly (3-hydroxybutyrate-co-4-hydroxybutyrate) films incorporating thyme essential oil for active packaging of white bread, Food Control 133 (2022) 1–12, https://doi.org/10.1016/j.foodcont.2021.108688.
[71] A. Fraj, F. Jaâfar, M. Marti, L. Coderch, N. Ladhari, A comparative study of oregano (Origanum vulgare L.) essential oil-based polycaprolactone nanocapsules/microspheres: preparation, physicochemical characterization, and storage stability, Ind Crops Prod 140 (2019) 1–19, https://doi.org/10.1016/j.indcrop.2019.111669.
[72] W. Lu, M. Chen, M. Cheng, X. Yan, R. Zhang, R. Kong, J. Wang, X. Wang, Development of antioxidant and antimicrobial bioactive films based on oregano essential oil/mesoporous nano-silica/sodium alginate, Food Packag Shelf Life 29 (2021) 1–11, https://doi.org/10.1016/j.fpsl.2021.100691.
[73] T. Elo, V.S. Parihar, A. Bera, F. Javanshour, M. Kellomäki, R. Layek, Mechanically robust, transparent, and UV-shielding composite of Na-alginate and maleic acid-functionalized boron nitride nanosheets with improved antioxidant property, Colloids Surf. B Biointerfaces 233 (2024) 1–9, https://doi.org/10.1016/j.colsurfb.2023.113641.
[74] A.O. Orisawayi, P. Boylla, K.K. Koziol, S.S. Rahatekar, Sustainable wet-spun cellulose-Moringa oleifera composite fibres for potential water purification, RSC Adv. 15 (2025) 17730–17745, https://doi.org/10.1039/D5RA02386F.
[75] D.N. Iqbal, A. Ashraf, A. Nazir, S.Z. Alshawwa, M. Iqbal, N. Ahmad, Fabrication, properties, and stability of oregano essential oil and sodium alginate-based wound-healing hydrogels, Dose-Response 21 (2023) 1–15, https://doi.org/10.1177/15593258231204186.
[76] S. Gholamian, M. Nourani, N. Bakhshi, Formation and characterization of calcium alginate hydrogel beads filled with cumin seeds essential oil, Food Chem. 338 (2021) 1–10, https://doi.org/10.1016/j.foodchem.2020.128143.
[77] Z. Riahi, A. Khan, J.-W. Rhim, G.H. Shin, J.T. Kim, Carbon dots-functionalized polyaniline incorporated into sodium alginate/cellulose nanofibrils film for sustainable intelligent and active packaging of shrimp, Sustain. Mater. Technol. 43 (2025) 1–16, https://doi.org/10.1016/j.susmat.2024.e01217.
[78] C. Yadav, M. Chhajed, P. Choudhury, R.P. Sahu, A. Patel, S. Chawla, L. Goswami, C. Goswami, X. Li, A.K. Agrawal, A. Saini, P.K. Maji, Bio-extract amalgamated sodium alginate-cellulose nanofibres based 3D-sponges with interpenetrating BioPU coating as potential wound care scaffolds, Mater. Sci. Eng. C 118 (2021) 1–18, https://doi.org/10.1016/j.msec.2020.111348.
[79] I. Zaets, O. Podolich, O. Kukharenko, G. Reshetnyak, S. Shpylova, M. Sosnin, L. Khirunenko, N. Kozyrovska, J.-P. de Vera, Bacterial cellulose may provide the microbial-life biosignature in the rock records, Adv. Space Res. 53 (2014) 828–835, https://doi.org/10.1016/j.asr.2014.01.002.
[80] Q. Li, M. Duan, D. Hou, X. Chen, J. Shi, W. Zhou, Fabrication and characterization of Ca(II)-alginate-based beads combined with different polysaccharides as vehicles for delivery, release and storage of tea polyphenols, Food Hydrocoll. 112 (2021) 1–10, https://doi.org/10.1016/j.foodhyd.2020.106274.
[81] Y. Liu, J.-C. Zhao, C.-J. Zhang, L. Cui, Y. Guo, P. Zhu, H. Zhang, Z.-W. Zheng, D.-Y. Wang, Flame retardancy and thermal degradation properties of cotton/alginate

fabric, J. Therm. Anal. Calorim. 127 (2017) 1543–1551, https://doi.org/10.1007/s10973-016-5418-6.
[82] Z. Yao, Y. Qian, Y. Jin, S. Wang, J. Li, W.-E. Yuan, C. Fan, Biomimetic multilayer polycaprolactone/sodium alginate hydrogel scaffolds loaded with melatonin facilitate tendon regeneration, Carbohydr. Polym. 277 (2022) 1–12, https://doi.org/10.1016/j.carbpol.2021.118865.
[83] A. Salama, M. Hasanin, P. Hesemann, Synthesis and antimicrobial properties of new chitosan derivatives containing guanidinium groups, Carbohydr. Polym. 241 (2020) 1–8, https://doi.org/10.1016/j.carbpol.2020.116363.
[84] D.N. Iqbal, A. Ashraf, A. Nazir, S.Z. Alshawwa, M. Iqbal, N. Ahmad, Fabrication, properties, and stability of oregano essential oil and sodium alginate-based wound-healing hydrogels, Dose-Response 21 (2023) 1–15, https://doi.org/10.1177/15593258231204186.
[85] M. Chelu, Hydrogels with essential oils: recent advances in designs and applications, Gels 10 (2024) 1–31, https://doi.org/10.3390/gels10100636.
[86] G. Tkalec, R. Kranvogl, A. Perva Uzunalić, Ž. Knez, Z. Novak, Optimisation of critical parameters during alginate aerogels' production, J. Non Cryst. Solids 443 (2016) 112–117, https://doi.org/10.1016/j.jnoncrysol.2016.04.014.
[87] T.H. Aneem, S.Y. Wong, H. Afrin, M. Nurunnabi, X. Li, M.T. Arafat, Investigation of coagulation process of wet-spun sodium alginate polymannuronate fibers with varied functionality using organic coagulants and cross-linkers, Mater Today Chem 22 (2021) 1–15, https://doi.org/10.1016/j.mtchem.2021.100580.
[88] M.J. Paris, N. Ramírez-Corona, E. Palou, A. López-Malo, Modelling release mechanisms of cinnamon (Cinnamomum zeylanicum) essential oil encapsulated in alginate beads during vapor-phase application, J. Food Eng. 282 (2020) 1–9, https://doi.org/10.1016/j.jfoodeng.2020.110024.
[89] S.M. Hosseini, H. Hosseini, M.A. Mohammadifar, A.M. Mortazavian, A. Mohammadi, K. Khosravi-Darani, S. Shojaee-Aliabadi, S. Dehghan, R. Khaksar, Incorporation of essential oil in alginate microparticles by multiple emulsion/ionic gelation process, Int. J. Biol. Macromol. 62 (2013) 582–588, https://doi.org/10.1016/j.ijbiomac.2013.09.054.
[90] S. Noppakundilograt, P. Piboon, W. Graisuwan, R. Nuisin, S. Kiatkamjornwong, Encapsulated eucalyptus oil in ionically cross-linked alginate microcapsules and its controlled release, Carbohydr. Polym. 131 (2015) 23–33, https://doi.org/10.1016/j.carbpol.2015.05.054.
[91] H. Nasution, H. Harahap, E. Julianti, A. Safitri, M. Jaafar, Smart packaging based on polylactic acid: the effects of antibacterial and antioxidant agents from natural extracts on physical–mechanical properties, colony reduction, perishable food shelf life, and future prospective, Polymers (Basel) 15 (2023) 4103.
[92] R. Parkale, P. Pulugu, P. Kumar, Nanomaterials Decoration on Commercial Cotton Bandages for Pain and Infection Management, 2021.
[93] L. Vimercati, D. Cavone, A. Caputi, L. De Maria, M. Tria, E. Prato, G.M. Ferri, Nanoparticles: an experimental study of zinc nanoparticles toxicity on marine crustaceans. General overview on the health implications in humans, Front Public Health 8 (2020) 1–19, https://doi.org/10.3389/fpubh.2020.00192.
[94] H. Bagheri Darvish, A. Bahrami, S.M. Jafari, L. Williams, Micro/nanoencapsulation strategy to improve the efficiency of natural antimicrobials against *Listeria monocytogenes* in food products, Crit. Rev. Food Sci. Nutr. 61 (2021) 1241–1259, https://doi.org/10.1080/10408398.2020.1755950.
[95] Q. Qiu, S. Chen, Y. Li, Y. Yang, H. Zhang, Z. Quan, X. Qin, R. Wang, J. Yu, Functional nanofibers embedded into textiles for durable antibacterial properties, Chem. Eng. J. 384 (2020) 1–9, https://doi.org/10.1016/j.cej.2019.123241.



https://dspace.org/

Deposition of alginate-oregano nanofibres on cotton gauze for potential antimicrobial applications

Orisawayi, Abimbola Oluwatayo; Lu, Hao; Badruddin, Ishrat Jahan; Venkatraman, Prabhuraj D.; Britten, Nicole S. ...

2025-08-01
Elsevier
https://doi.org/10.1016/j.ijbiomac.2025.145372
Orisawayi AO, Lu H, Badruddin IJ, et al., (2025) Deposition of alginate-oregano nanofibres on cotton gauze for potential antimicrobial applications. International Journal of Biological Macromolecules, Volume 319, Part 1, August 2025, Article number 145372

Downloaded from a DSpace repository. https://dspace.org/